

# Monitoring the COVID-19 epidemic with nationwide telecommunication data

Joel Persson<sup>\*†</sup>

Jurriaan F. Parie\*

Stefan Feuerriegel\*

## Abstract

In response to the novel coronavirus disease (COVID-19), governments have introduced severe policy measures with substantial effects on human behavior. Here, we perform a large-scale, spatio-temporal analysis of human mobility during the COVID-19 epidemic. We derive human mobility from anonymized, aggregated telecommunication data in a nationwide setting (Switzerland; February 10–April 26, 2020), consisting of  $\sim 1.5$  billion trips. In comparison to the same time period from 2019, human movement in Switzerland dropped by 49.1 %. The strongest reduction is linked to bans on gatherings of more than 5 people, which is estimated to have decreased mobility by 24.9 %, followed by venue closures (stores, restaurants, and bars) and school closures. As such, human mobility at a given day predicts reported cases 7–13 days ahead. A 1 % reduction in human mobility predicts a 0.88–1.11 % reduction in daily reported COVID-19 cases. When managing epidemics, monitoring human mobility via telecommunication data can support public decision-makers in two ways. First, it helps in assessing policy impact; second, it provides a scalable tool for near real-time epidemic surveillance, thereby enabling evidence-based policies.

**Keywords:** COVID-19, epidemiology, human mobility, telecommunication data, Bayesian modeling

---

<sup>\*</sup>ETH Zurich (Swiss Federal Institute of Technology), 8092 Zurich, Switzerland

<sup>†</sup>[jpersson@ethz.ch](mailto:jpersson@ethz.ch)

# 1 Introduction

The novel coronavirus disease (COVID-19) has evolved into a global pandemic, which, as of December 15, 2020, has been responsible for more than 70 million reported cases<sup>1</sup>. In response, governments around the world have put policy measures into effect with the aim of reducing transmission rates<sup>2–6</sup>. Examples of policy measures are border closures, school closures, venue closures, and bans on gatherings.

Prior literature has suggested the use of human mobility data to model the COVID-19 epidemic<sup>7</sup>. Mobility patterns have been inferred from point-of-interest (POI) check-ins<sup>8–12</sup> and from location logs of smartphone apps<sup>13–25</sup>. Other works have used telecommunication data to model spreading patterns<sup>26,27</sup> and for exploratory analysis of mobility patterns<sup>28–30</sup> but none have yet empirically explored the link between mobility and policy measures. Establishing such a link would provide a scalable tool for near real-time disease surveillance under policy measures and, in particular, enable evidence-based policies. Previously, the value of telecommunication data for disease surveillance has been studied in the context of malaria<sup>31,32</sup>, influenza<sup>33</sup>, and other infectious diseases<sup>34–36</sup>, where the objective was to make spatio-temporal forecasts. In contrast, this paper demonstrates the utility of telecommunication data for near real-time assessments of COVID-19 policies. In fact, nationwide data from mobile telecommunication networks has been used by governments during the first wave of COVID-19<sup>37</sup>. However, to the best of our knowledge, empirical evidence regarding the effectiveness of telecommunication data for epidemic surveillance in the context of COVID-19 is absent.

In this paper, we analyze human mobility during the COVID-19 epidemic. Our analysis is based on large-scale, granular data of human movements (anonymized and aggregated) consisting of  $\sim 1.5$  billion trips in Switzerland during the first COVID-19 wave (February 10–April 26, 2020) derived from telecommunication data. Using regression models, we estimate the (1) impact of policy measures on human mobility, and (2) how mobility predicts the growth in reported COVID-19

cases. By establishing that policy measures reduce mobility and that mobility predicts reported cases, mobility insights can be used to inform when to implement policy measures. The findings are therefore of direct value to public decision-makers: monitoring human mobility through telecommunication data provides an effective and scalable tool for near real-time epidemiology and thus, management of the COVID-19 epidemic.

To establish the ability of telecommunication data for near real-time monitoring of the COVID-19 epidemic, we follow a two-stage approach (see [Methods](#)). We first study the reduction in mobility due to 5 different policy measures (bans on gatherings of more than 100 people, bans on gatherings of more than 5 people, school closures, venue closures, and border closures). We then estimate to what extent the reduction in mobility predicts decreases in reported case growth. Here, we compare the predictive ability over a forecast window from 7 to 13 days. Taken together, the results confirm the effectiveness of policy measures for reducing human mobility and, in turn, human mobility as a predictor of reported cases by a lead time of approx. 7–13 days. The two-stage approach is repeated for total trips; 3 different modes of mobility (train, road, highway); and 2 different purposes for mobility (commuters vs. non-commuters). In an extended analysis, we further perform a mediation analysis. Here, we decompose the reduction in new reported cases due to the policy measures into (a) the part that is only explained by reductions in mobility and (b) the part that is explained by other behavioral adaptations.

## Results

### **Human mobility derived from nationwide telecommunication data**

We analyze large-scale data on human mobility during February 10–April 26, 2020 from Switzerland. For this, human movements were derived from telecommunication data (see [Methods](#)). Telecommunication data provide more reliable and extensive information on mobility compared

to alternative data sources (check-ins or location logs from smartphone apps)<sup>7,38,39</sup>. In particular, our telecommunication data represents routine signal exchanges (“pings”) exchanged between mobile devices and network antennas. These were recorded for all mobile devices in Switzerland regardless of the mobile service provider. Based on the telecommunication data, granular locations (longitude, latitude) of individuals carrying a mobile device were inferred. This yields data on micro-level movements from all mobile devices in a nationwide setting. Altogether, the nationwide mobility for a population of  $\sim$ 8.6 million people was estimated.

For the analysis, the telecommunication data were then processed to compute the number of trips between postal codes per day and canton. All trips were further classified according to the mode of mobility (“train”, “highway”, and other “road” movements) and purpose (“commuting” vs. “non-commuting”). For the time period of this study (February 10–April 26, 2020), our data include a total of  $\sim$ 1.5 billion trips. Details are reported in [Methods](#).

We further collected data on the use of policy measures in Switzerland. Switzerland comprises 26 member states at the sub-national level (called “cantons”), each with a large degree of sovereignty. As a result, the use of policy measures varies across cantons with respect to their order and timing in a way that is similar to the variation among other European countries. Some cantons (e. g., Ticino at the border to Italy and Geneva at the border to France) showed epidemiological dynamics with large numbers of reported cases and responded with comparatively stringent policy measures during the first wave of COVID-19. Other cantons had lower case numbers and put policy measures in effect during a later phase of the epidemic. We followed a systematic procedure (see [Supplement A](#)) based on which we encoded policy measures according to five categories: bans on gatherings ( $> 100$  people), bans on gatherings ( $> 5$  people), school closures, venue closures (stores, restaurants, bars), and border closures. The implementation dates of the chosen policy measures varied greatly across cantons (but then remained in effect for the complete study period, i. e., until April 10).

The spatio-temporal patterns of human movements in our data are as follows. Overall, we

recorded  $\sim$ 95 million trips in the first week (February 24–March 1, 2020), during which all five policy measures were in effect in all 26 cantons. In comparison, the same time period in 2019 (as a reference period) registered  $\sim$ 186 million trips. This amounts to a reduction of 49.1 %. The reduction occurred in all cantons (Figure 1a,b). The highest decline was observed in Ticino and Geneva, which are located at the borders with Italy and France, respectively. Both cantons also reported the highest number of COVID-19 cases.

The largest mobility reduction compared to 2019 occurred on Sunday, March 22, 2020 (Figure 1c). In comparison to Sunday, March 24, 2019, the reduction in trip counts ranged between 49.3 % and 77.0 % across the 26 cantons (mean: 61.6 % reduction per canton). Overall, the reduction in mobility is of similar magnitude for both rural (e. g., canton of Valais) and urban regions (e. g., cantons of Basel-City and Zurich). Furthermore, movements declined for all modes of mobility (Figure 1d) and for all purposes (Figure 1e). After the implementation of the policy measures, trips by train remained low for the rest of the study period, while highway traffic was on an upward trend (Figure 1d). Similarly, trips by commuters remained at a low level after the implementation of the policy measures, whereas trips not for commuting (i. e., personal purposes) started increasing in early April (Figure 1e).

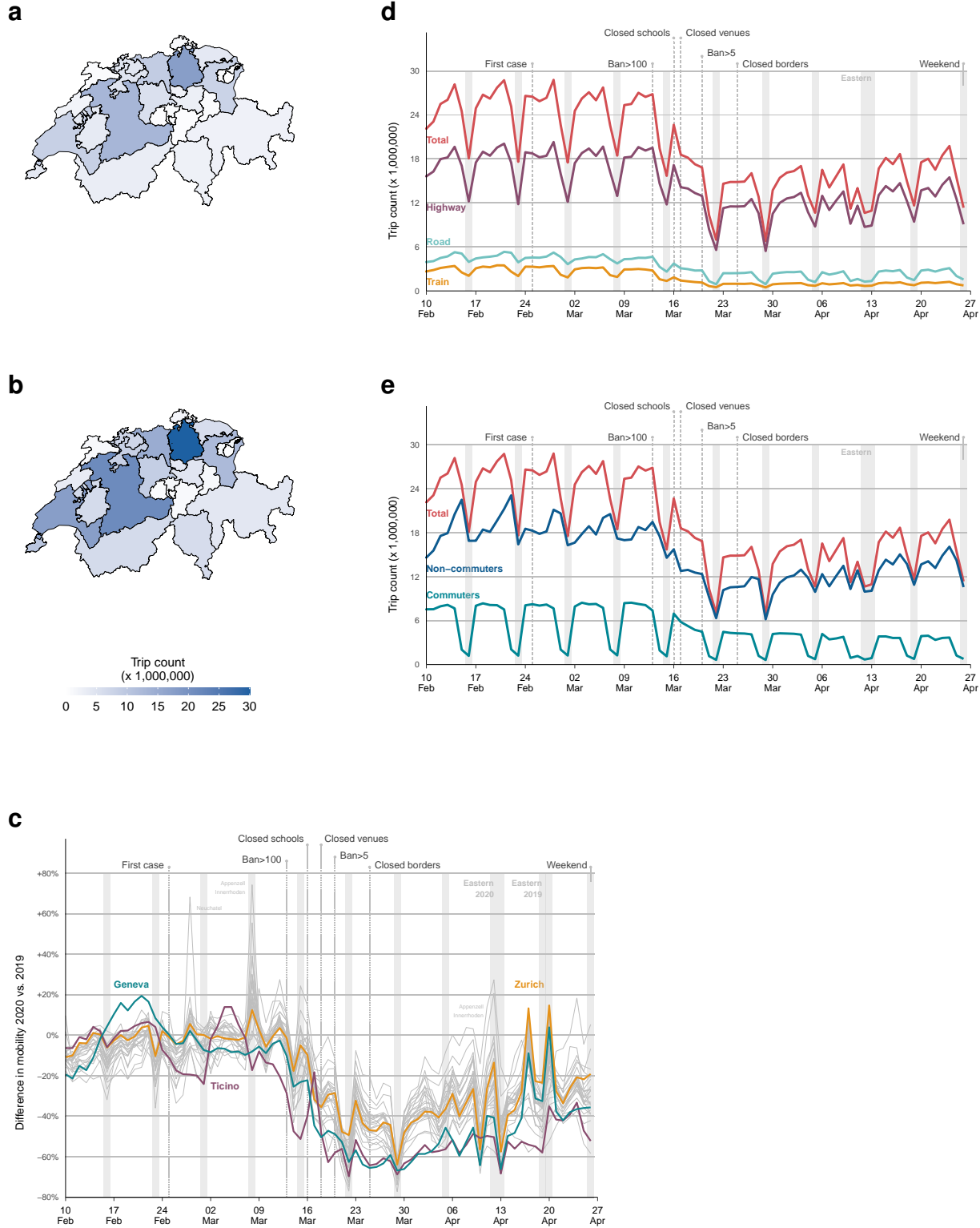


**Figure 1:** Nationwide human mobility in Switzerland during the first wave of the COVID-19 epidemic. Mobility is quantified by movements (“trips”) between different post code areas. **(a)** Total number of trips per canton for the first week after all policy measures were put in effect in all cantons (March 25–April 1, 2020). **(b)** Total number of trips for the same week in 2019 (i. e., as reference year). For this week, the total number of trips dropped from ~186 million (in 2019) to ~95 million (in 2020), i. e., a reduction of 49.1 %. **(c)** Percentage change in total trips across 26 sub-national levels (cantons) for 2020 vs. 2019 (when aligned for day-of-week patterns). The reason for the comparison to 2019 is to show the reduction in mobility relative to a reference year, while accounting for seasonal changes in mobility. A higher reduction in mobility is observed for cantons that also reported a high number of COVID-19 cases (i. e., Ticino and Geneva). **(d)** Reduction in trip count by mode of mobility. **(e)** Reduction in trip count by purpose of mobility. Annotations show nationwide implementation dates of policy measures (implementation dates at cantonal level are reported in [Supplement A](#)).

## Estimating the reduction in human mobility due to policy measures

We estimate the reduction in mobility due to the policy measures with a regression model. The estimates are identified via a difference-in-difference analysis and may thus be given a causal interpretation under certain assumptions (see Supplement B.1).

The most effective policies for reducing trip counts are as follows (Figure 2a). Based on our model, bans on gatherings of more than 5 people reduced total trips by 24.9 % (95 % credible interval [CrI]: 22.1–27.6 %), venue closures reduced total trips by 22.3 % (95 % CrI: 15.6–29.0 %), and school closures reduced total trips by 21.6 % (95 % CrI: 17.9–25.0 %). For a precise ranking, the width of the credible intervals must be considered. Here, the aforementioned policy measures appear more effective at reducing total trips than the other two policy measures (i. e., bans on gatherings of more than 100 and border closures). In particular, bans on gatherings of more than 100 people are linked to a comparatively smaller change in total trips than bans on gatherings of more than 5 people (i. e., the 95 % CrIs of the estimates are disjoint). For border closures, the credible interval includes zero. Overall, policy measures are important determinants of mobility reductions during the COVID-19 epidemic.

The estimated mobility reduction depends on the underlying mode (Figure 2b). Across all policy measures, the mobility reduction is more pronounced for highways than for road movements. This observation is to be expected. Highways are often used for long-distance travel, which is more likely to be suspended during an epidemic, while roads also include movements within close proximity and are more likely to correspond to routine or essential activities (e. g., grocery shopping). For the ban on gatherings and school closures, the largest reduction is seen in trips by train, which can be explained by the widespread use of public transportation in Switzerland. Finally, we observe a wide credible interval for the estimated effect of venue closures on trips by train. A potential reason for this is that the use of trains (e. g., for visiting stores) varies across cantons, as some cantons (e. g., Zurich) have a high population density with extensive shopping infrastructure, while others (e. g., Appenzell Innerrhoden) have only a few stores due to their low population

density, resulting in the need for travel to visit stores.

The estimated effect sizes are fairly similar for trips made for commuting versus non-commuting (Figure 2c). This is interesting considering that no policy measure in Switzerland directly prohibited movement to and from work. The efficacy of border closures is uncertain since the credible interval for its estimated effect includes zero. In contrast, a negative effect is observed for commuting. Here, one potential reason is that border closures have reduced the number of cross-border commuters.

The findings are robust to alternative model specifications (see the robustness checks in Supplement D). Specifically, changing the specification of time-related control variables still gives parameter estimates for the policy measures that imply decreases in mobility.

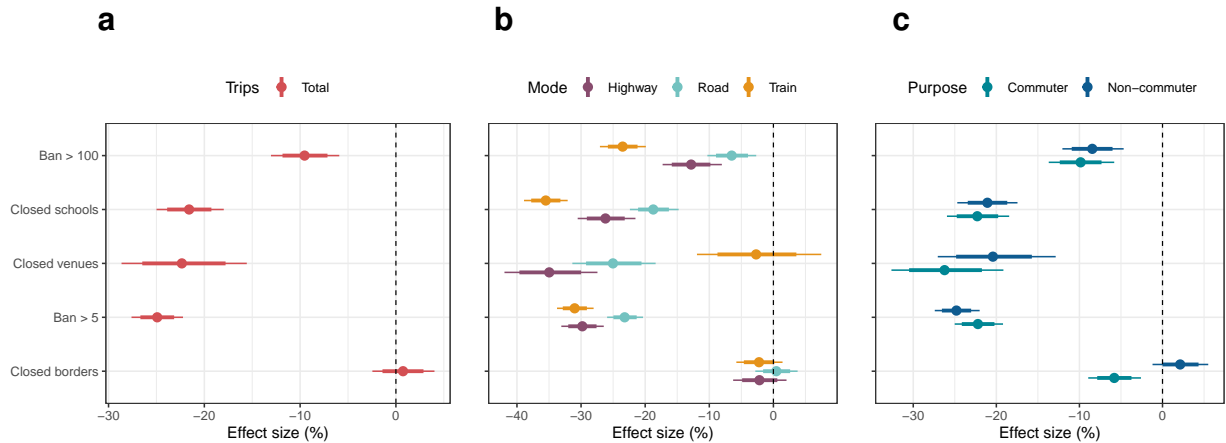


Figure 2: The estimated effects of policy measures on mobility. Shown are the estimated effects on (a) the total number of trips, (b) trips by mode, and (c) trips by purpose. The dots in (a)–(c) show posterior means; the thick and thin bars represent the 80 % and 95 % credible intervals, respectively. Policy measures are arranged from top to bottom in the order in which they were implemented (cf. Supplement A).

## Estimating the relationship between mobility and COVID-19 cases

The epidemic dynamics during the first wave of COVID-19 in Switzerland are as follows. The initial exponential growth rates exhibit considerable heterogeneity across cantons (Figure 3a). The strongest initial growth is observed for the cantons Ticino and Geneva, resulting in the largest

number of cases towards the end of the sample. Moreover, the number of reported cases at the dates that policy measures were implemented varies greatly across cantons (Figure 3b). This reflects different responses among cantons to local infection dynamics.

We use regression models to estimate the extent to which decreases in mobility predict future reductions in the reported number of new cases (Figure 3c). The predicted decrease is studied with a forecast window over 7–13 days. The forecast window is set analogous to previous research<sup>25</sup>, and so that it covers variations in incubation time combined with reporting delay.

We find that decreases in mobility at a given day predict decreases in reported new cases 7 to 13 days later. For a 7-day ahead forecast, we find that a 1 % decrease in the total number of trips predicts a 0.88 % (95 % CrI: 0.7–1.1 %) reduction in the reported number of new cases. For a 13-day ahead forecast, a 1 % decrease in the total number of trips predicts a 1.11 % (95 % CrI: 0.9–1.6 %) reduction in the reported number of new cases. Overall, mobility predicts decreases in the reported number of new cases over the whole forecast horizon. The predicted decrease is larger for longer forecasts. This result is to be expected, as a longer time window accommodates the full distribution of incubation periods (plus reporting delays). Altogether, the regression analysis provides evidence of that mobility predicts epidemic dynamics.

Our analysis also shows that the predicted change in the reported number of new cases varies across the mode and purpose of trips. In terms of mode, decreases in trips by highway and train predict reductions in the reported number of new cases of similar magnitude (Figure 3d). Their estimates have comparatively narrow credible intervals, reflecting a higher degree of certainty. Trips are also categorized according to their purpose, namely commuting vs. non-commuting. The results show that decreases in trips for commuting predict smaller reductions in the number of reported new cases compared to decreases in non-commuting trips (Figure 3e). Predicted reductions are nonetheless found for both modes of mobility (i. e., commuting vs. non-commuting), all categories of purpose (i. e., highway, road, and train), and for the whole 7–13 day forecast window. Again, a larger reduction is predicted for longer forecasts.

The predictive ability of mobility for reported new cases holds with alternative model specifications (see the robustness checks in Supplement D). For most of the 7–13 day forecasts, changing how we control for time-related factors still results in a predicted decrease in reported cases given decreases in mobility.

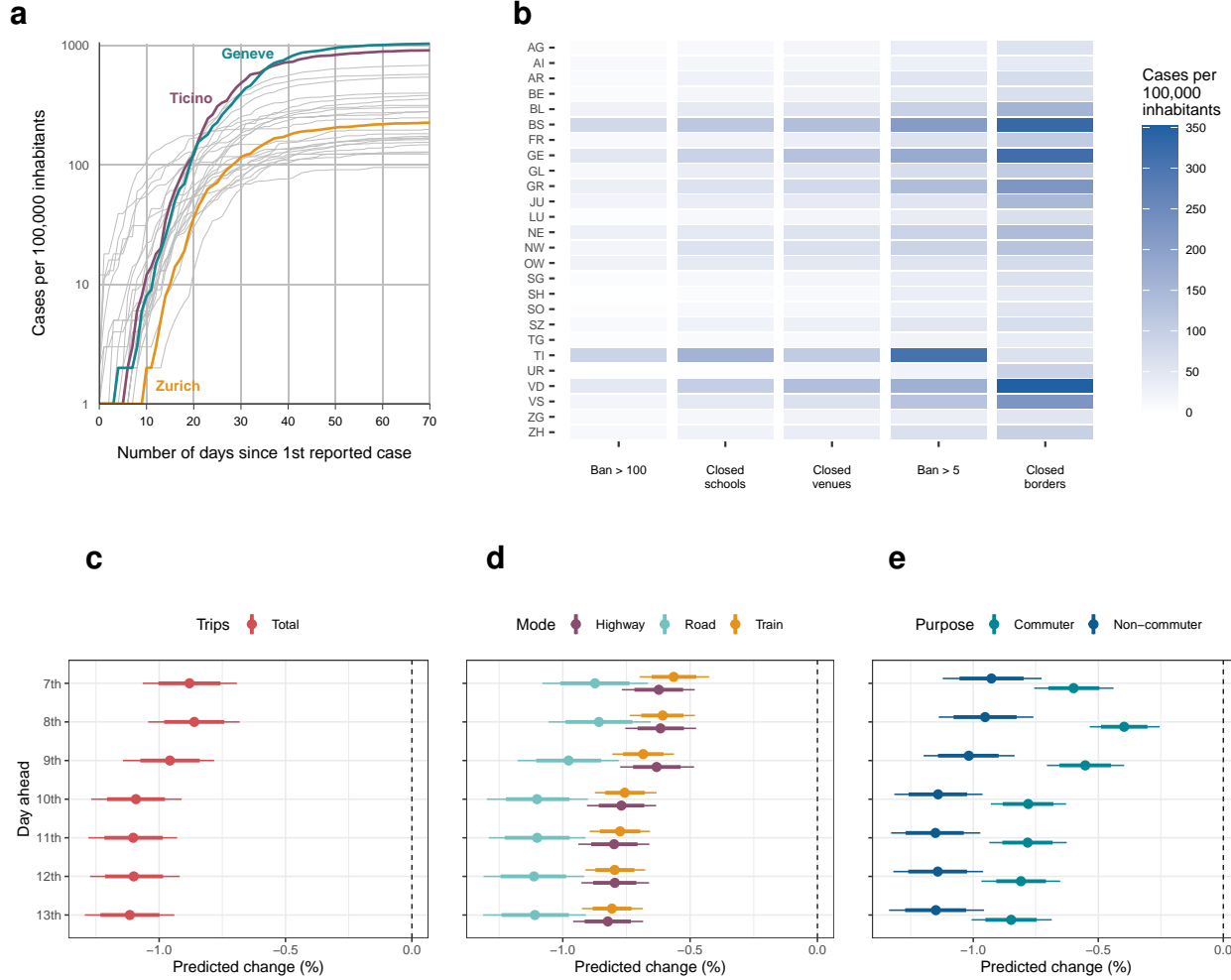


Figure 3: Decreases in human mobility predicts reductions in reported cases of COVID-19 over a forecast window of 7–13 days. **(a)** COVID-19 case growth since the 1st reported case for 26 Swiss cantons. **(b)** Number of COVID-19 cases when the policy measures were implemented for all 26 Swiss cantons. Shown are abbreviated names. The predicted change in reported new COVID-19 cases at a given day is based on mobility lagged by 7 days to 13 days. The predicted change is reported given a 1 % decrease in **(c)** total trips, **(d)** mode, and **(e)** purpose. Posterior means are shown as dots, while 80 % and 95 % credible intervals are shown as thick and thin bars, respectively.

## Estimating the mediating role of mobility

In an extended analysis, we study how decreases in reported case growth is explained by reductions in mobility due to policy measures versus other behavioral changes due to policy measures. The estimates are obtained from a mediation analysis that decomposes the total effects of the policy measures on reported case growth into (1) their direct effects not explained by changes in mobility and (2) their indirect effects through mobility. The mediation analysis is performed by combining our two regression models into a structural equation model (see Supplement F for details). Results from mediation analysis are reported for the total number of trips.

The mediation analysis shows a large direct effect for bans on gatherings of more than 5 people, bans on gatherings of more than 100 people, and school closures (4). Pronounced indirect effects are found for all policy measures. In particular, the indirect effect of venue closures makes up about a third of their total effect at several lags. Moreover, border closures are estimated to only have reduced the reported number of new cases indirectly through mobility. The results are discussed in further detail in Supplement F. In summary, the results show that mobility is an important mediator: the studied policy measures operate – to a large degree – through mobility. Thus, policy measures aimed at reducing mobility appear to be effective for reducing COVID-19 case growth.

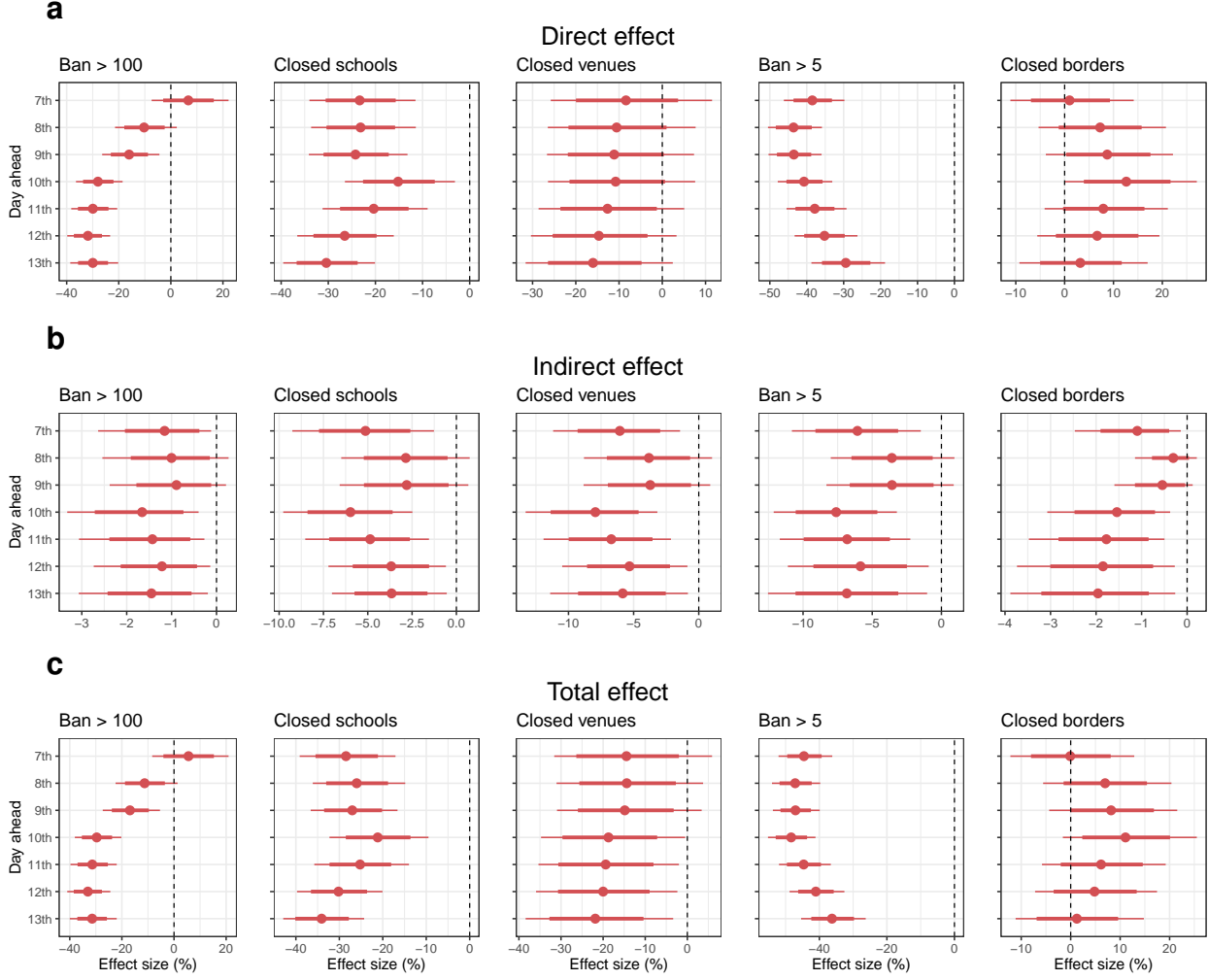


Figure 4: Mobility mediates the effect of policy measures on the reported number of new cases. Estimated **(a)** direct effect of policy measures, **(b)** indirect effect of policy measures via total trips, and **(c)** total effect of policy measures on the 7th to 13th day ahead. Posterior means are shown as dots, while 80 % and 95 % credible intervals are shown as thick and thin bars, respectively. Policy measures are arranged from top to bottom in the order in which they were implemented (cf. Supplement A).

## Discussion

This study shows the ability of telecommunication data for near real-time monitoring of the COVID-19 epidemic. Our analysis is based on nationwide telecommunication data during February 10–April 26, 2020 from Switzerland, which were used to infer nationwide mobility patterns.

This supports monitoring of the COVID-19 epidemic as follows: (1) We first studied the link between policy measures and human mobility. In particular, we performed a difference-in-difference quantifying how mobility was reduced due to 5 different policy measures (bans on gatherings, school closures, venue closures, and border closures). The largest reduction in total trips was linked to bans on gatherings of more than 5 people, followed by venue closures and school closures. Overall, the policy measures resulted in substantial reductions of human mobility. (2) We then studied the link between human mobility and reported COVID-19 cases. Reductions in mobility predicted decreases in the number of reported new cases. Specifically, a reduction in human movement by 1 % predicted a 0.88–1.11 % reduction in the daily number of new cases of COVID-19 over a forecast horizon of 7 days to 13 days. Our modeling approach with telecommunication data therefore provides near real-time insights for disease surveillance. Taken together, the findings enable quantitative comparisons of the extent to which policy measures reduce mobility and, subsequently, reduce reported cases of COVID-19.

The use of telecommunication data for nationwide monitoring has several benefits<sup>7,40</sup>. First, telecommunication data from mobile networks provide comprehensive coverage. Specifically, such data capture all movements of individuals carrying mobile devices without explicit user interaction, including those from non-residential and even foreign individuals. Mobile devices routinely exchange information when searching for signals from adjacent antennas; hence, metadata are retrieved regardless of the underlying mobile service provider. Second, such metadata can be collected in an anonymized manner that is compatible with data privacy laws. Third, movements at a micro-level (e. g., trips to other households, school, and work) can be inferred. Thus, compared to alternative sources of mobility information such as check-ins or smartphone apps, telecommunication data are considered to be more complete<sup>7,38,39</sup>. Fourth, unlike smartphone apps, telecommunication data are also available in low-income countries<sup>41</sup>. Finally, telecommunication data are measured with high frequency (e. g., daily), thereby enabling regularly updated monitoring as needed by decision-makers. Based on these benefits, telecommunication data appear to be highly

effective for policy monitoring during the COVID-19 epidemic.

This work is subject to the typical limitations of observational studies. First, the findings depend on the accuracy of the data on COVID-19 cases. Second, our models are informed by recommendations for COVID-19 modeling<sup>42</sup> and, therefore, follow parsimonious specifications to isolate features of the epidemic for policy-relevant insights. We cannot, however, rule out the possibility that there exist external factors beyond those that are captured by the spatially and temporally varying variables in the models. To address this, we use flexible models and conduct extensive robustness checks (Supplement D). Third, the model linking policy measures to mobility estimates effects, while the model linking mobility to cases is predictive. The different objectives of the models address the needs of public decision-makers: the former serves policy assessments and the latter epidemiological forecasting, respectively. Therefore, the estimates from the former are identified with a difference-in-difference analysis and may thus warrant causal interpretations under certain assumptions (see Supplement B.1). On the other hand, the estimates from the latter are conditional associations since the model does not control for that policy measures reduce both mobility and cases. Therefore, the latter model predicts decreases in reported cases from reductions in mobility when both reductions are driven by policy measures (see Supplement B.2 for a discussion of this approach). Fourth, our findings are limited to our study setting, that is, the first wave in Switzerland. Future research may confirm the external validity of our findings by analyzing other countries or time periods.

Inferring mobility patterns from telecommunication data is inherently coupled to the coverage of such data and our definition of trips. Only movements for individuals who carry a mobile device with a SIM card are included. In particular, trips are not included for individuals who do not carry SIM cards. Similarly, trips may be counted several times if an individual carries several SIM cards (e.g., when carrying both a phone and a SIM-based tablet). It is also possible that trips by children, elderly, or other parts of the population with less phone usage are underrepresented in the data. Furthermore, micro-level movements are not observed but recovered via triangulation

between antennas through the use of a positioning algorithm achieving state-of-the-art accuracy. In spite of these limitations, telecommunication data are considered to be scalable and, in particular, more complete for inferring mobility patterns compared to alternative data sources<sup>7,38,39</sup>. Moreover, our objective is not to obtain accurate estimates of mobility in itself, but to evaluate the predictive ability of telecommunication data for reported case growth. Our analysis confirms telecommunication data as such a monitoring tool.

Our findings are of direct value for public decision-makers. Nationwide mobility data from mobile telecommunication networks can be leveraged for the management of epidemics. Thereby, we fill a previously noted void in the case of COVID-19<sup>38,39,43</sup>. Specifically, monitoring mobility supports public decision-makers when managing the COVID-19 epidemic in two ways. First, it helps public decision-makers in assessing the impact of policy measures targeted at mobility behavior. Second, by predicting epidemic growth, it provides a scalable tool for near real-time epidemic surveillance. Such tools are relevant for evidence-based policy-making of public authorities in the current COVID-19 epidemic.

## Methods

The aim of this study is to make population inference from nationwide telecommunication data. In our study, telecommunication data are collected from routine signal exchanges (i. e., pings) with antennas, regardless of the actual service provider. Based on the telecommunication data, mobility estimates are inferred as follows (Fig. 5): (1) Telecommunication data are collected at the level of antenna. (2) Telecommunication data at antenna level are used to infer micro-level movements of individuals via triangulation. (3) Data on micro-level movements are used to count movements between postal codes (named “trips”) over time. This procedure is performed to capture mobility levels in the population. (4) The data are further aggregated at the cantonal level per day in order to link them to policy measures and COVID-19 case numbers. The procedure is detailed in the following.

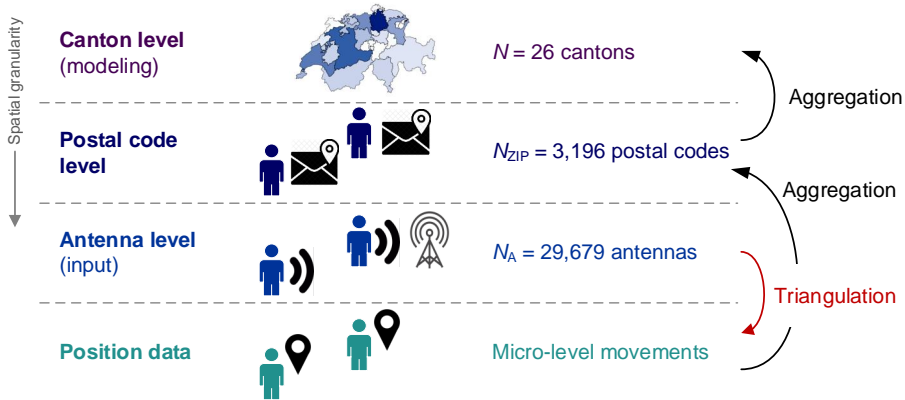


Figure 5: Deriving mobility estimates from nationwide telecommunication data for monitoring the COVID-19 epidemic.

## Nationwide telecommunication data

Telecommunication data are routinely collected from signal exchanges (i. e., pings) between mobile devices and adjacent antennas. Such signal exchanges occur for all SIM-based mobile devices (e. g., mobile phones, smartphones), regardless of the actual service provider. In particular, our

data also include movements of people with a foreign SIM card and, hence, represents nationwide telecommunication. A network event between a mobile device and mobile network compromises metadata as follows: the IMSI number of the SIM card, the date and time the SIM card connected to the mobile network, and the ID of the mobile antenna to which the SIM card was connected. The IMSI number is available for all SIM cards and thus represents a unique identifier, independent of the actual service provider. The events from mobile networks are extracted from the mobile communications systems every night, and thus the mobile data is available the following day. In our analysis, we use telecommunication metadata collected according to the above description by Swisscom<sup>44</sup>. Swisscom also ensured that IMSI numbers are stored in an anonymized format (see Ref. <sup>44</sup> for details).

Telecommunication data hold advantages over alternative data sources for the purpose of measuring human mobility. The advantages become especially clear in comparison to location data from check-ins<sup>8–12</sup> or location logs from smartphone apps<sup>13–20,45</sup>. First, compared to smartphone applications, SIM-based devices are fairly ubiquitous. This holds for both high-income countries (such as Switzerland) and low-income countries. Second, the use of telecommunication data ensures coverage for large parts of society. Specifically, it reduce the risk of an age bias (e.g., check-ins are known to be more frequent among younger, technology-savvy people). Third, telecommunication data avoid the need for user interaction with a device. Hence, many micro-level movements are captured (e.g., school visits, commuting to work, grocery shopping) that would otherwise not be subject to monitoring.

The telecommunication infrastructure operated by Swisscom has wide coverage<sup>44</sup>. Specifically, it covers 99.9% of the geographic area in Switzerland. The infrastructure records telecommunication metadata via almost 30,000 antennas. Hence, there are multiple antenna per postal code. In particular, approx. 7,000 of the antennas are of the GSM type, 11,000 of the UMTS type, and 12,000 of the LTE type<sup>46–48</sup>.

The frequency of pings is determined by the mobile device, occurring every time a mobile

phone connects to a new antenna or, if in between two antennas, every  $\sim 5$  minutes. Hence, the ping frequency produces data of higher temporal resolution than the data we later use for the analysis. An internal algorithm by Swisscom ensures that bouncing (i. e., when a phone bounces between antenna) is correctly addressed and attributed to a single antenna. The telecommunication metadata are then used to infer actual locations over time via triangulation (see next section).

## Inferring positions of SIM cards via triangulation

The locations of SIM cards within antenna areas are determined via triangulation between antennas through the use of a positioning algorithm<sup>49</sup>. A high-level description of the algorithm is as follows. Every signal from a SIM card in the telecommunication data is associated with a probability distribution over locations that represents the uncertainty of its actual location in a given antenna area at the time. The location is estimated from two random variables: the radius  $R$ , given by the distance of the signal from the origin of the antenna area, and its angle  $\Theta$  to the antenna azimuth. Here,  $R$  is Gaussian distributed with empirical mean and variance estimated via maximum likelihood, and  $\Theta$  follows a multinomial distribution depending only on the antenna azimuth and its bandwidth. The inferred locations are subject to a delay between signals between antennas and SIM cards. To address this, the location at a given point in time is estimated by marginalizing the probability distribution of the radius over the empirical distribution of signal delays estimated from all observations. Details are available in<sup>49</sup>. In sum, by tracking the location of SIM cards over time, we are able to capture micro-level movements of individuals.

The accuracy of the positioning algorithm has been empirically validated<sup>49</sup>. The median positioning error is 132 meters, making it highly accurate compared to state-of-the art methods<sup>50</sup>. The accuracy was determined by comparing the algorithm's predicted positions to self-reported actual positions for more than 6,000 trips with over 12,000 end-points<sup>49</sup>.

## Deriving mobility estimates from telecommunication data

Mobility has been frequently found to be helpful for understanding urban phenomena<sup>51,52</sup>. In this study, we derive mobility estimates from nationwide telecommunication data.

Trips are computed as follows. A single trip is defined as the movement of a SIM card between two different post code areas after the location has been static for 20 minutes. The trip is then counted for both post codes. Similarly, trips that cross midnight are counted for both days.

Post codes were chosen to define trips as they represent the smallest spatial unit that is officially defined by the federal government. Switzerland has 3,196 post code areas with high spatial granularity. The exact size varies between urban and rural regions, but, on average, a post code area in Switzerland covers merely 12.9 km<sup>2</sup>. Moreover, 71 % of the Swiss working population commute between different post codes for work and oftentimes even between cantons (<https://www.bfs.admin.ch/bfs/en/home/statistics/mobility-transport/passenger-transport/commuting.html>). The average (one-way) travel distance to work is 15.0 km (see previous URL), and, the average daily travel distance for leisure activities is 36.8 km (<https://www.bfs.admin.ch/bfs/en/home/statistics/mobility-transport/passenger-transport/travel-behaviour.html>). For both work and leisure activities, travel routinely spans several postal code areas. Hence, the use of nationwide telecommunication data combined with our definition of trips provides comparatively large-scale estimates of aggregate mobility.

For the analysis, daily trips were further aggregated as follows. First, each trip between post codes was mapped onto cantons at the sub-national level. Here, we used cantonal shape files from the Swiss government and aggregated all daily trips within each canton. Note that the number of trips into and out of cantons are captured with this aggregation due to the attribution of trips to both the departure and arrival post codes. The result of the aggregation is a panel (longitudinal) dataset of trip counts across cantons.

The reason for the aggregation to the cantonal level per day is twofold. First, policy measures

are implemented within cantons, and, second, COVID-19 case data are only published per day at the cantonal level. Therefore, data on policy measures and case number are not available on a more granular level.

Trips were further labeled according to both mode and purpose. The mode of trips was differentiated based on estimating the location of SIM cards with the positioning algorithm and the position of antennas along train, highway, and road networks. If several modes of mobility were used in the same trip, the mode with the longest leg was chosen. For comparison, public transport through train is an important mode of transportation in Switzerland (<https://www.bfs.admin.ch/bfs/en/home/statistics/mobility-transport/passenger-transport/travel-behaviour.html>) that is relevant for explaining the results. The purpose of mobility was classified based on trips to/from work (called “commuting”) and all other trips (called “non-commuting”). This differentiation was based on the home and work locations of individuals (i.e., postal code area). These locations were derived from the most frequent geographic location of individuals between 8 pm–8 am for home locations and 8 am–5 pm for work locations. Afterwards, both home and work location were matched against the departure and arrival (postal code area) of a trip to determine whether the trip was to/from work, and hence labeled “commuting”. The classification of trips into mode of transport is highly accurate. A validation against self-reported data was performed, showing that 90 % of all trips were correctly classified<sup>49</sup>.

## Modeling overview

In this section, we present the regression models used to estimate the relationship between (1) policy measures and mobility and (2) mobility and reported cases. Here, the first model estimates the reduction in mobility due to policy measures. The estimates are identified with a difference-in-difference analysis and may therefore be given a causal interpretation under certain assumptions (see Supplement B.1). The second model, in turn, estimates the extent to which reductions in

mobility predict decreases in the reported number of new cases as policy measures are being implemented.

The models have parsimonious specifications recommended for isolating policy-relevant insights<sup>42</sup> and are informed by epidemiology. In particular, they are formalized as Bayesian hierarchical negative binomial regression models. Rather than modeling the disease dynamics themselves (as with a compartment model), our focus is on estimating the relative effect of other determinants, namely, policy measures and mobility. The use of negative binomial distributions is common in epidemiological modeling, as it allows for overdispersion in dependent variable (i.e., the number of trips and the reported number of new cases). Furthermore, each model uses a log-link between the dependent and explanatory variables. For the model of the reported number of new cases, it enables us to capture the exponential growth in cases during the initial stages of an epidemic, also observed in our data. For the model of mobility, it makes the estimates relative to the observed levels of mobility. Both dependent variables were found to follow negative binomial distributions (with overdispersion). See Appendix C.4 for an analysis of overdispersion.

The models include further controls for (1) population size per canton, (2) unobserved heterogeneity between cantons, and (3) time effects as follows. (1) We control for differences in population size among cantons with an offset term. This is motivated by the fact that the magnitude of the estimated effects depend on the population size. Hence, the model estimates are relative to the number of inhabitants per canton. (2) Unobserved heterogeneity is estimated with a canton random effect. We thereby account for unobserved factors that affect both policy measures and mobility (for the former model) and mobility and cases (for the latter model). (3) Time effects are modeled in two ways. On the one hand, we include weekday fixed effects to control for variations in the implementation of policy measures, levels of mobility, and reporting/testing across weekdays (e.g., mobility is higher on weekdays, whereas testing is lower on weekends; thus, reported cases are lower on weekends and tests conducted on weekends may be reported on Mondays or Tuesdays). On the other hand, we incorporate a trend variable that controls for changes in case

dynamics or behavioral adaptations towards social distancing that occur over time since a canton first reported a case. This could for instance occur due to unobserved changes in adherence to other policy measures (e.g., wearing masks and keeping physical distance of at least 1.5 meters) over time. Here, we model the variation in when cantons reported their first case as potentially dependent on the unobserved canton heterogeneity.

The results with additional controls (e.g., test frequency, spatial correlation between cantons, and dependence between the different trip variables) are part of the robustness checks.

## Model for estimating the reduction in human mobility due to policy measures

A multiple time period, multiple group difference-in-difference (DiD) analysis<sup>53</sup> is conducted to estimate the effect of each policy measure on mobility. We restrict the analysis to the time period between February 24 and April 5, 2020; that is, starting before the first reported COVID-19 case in Switzerland and ending prior to Easter holidays. With this time period, the initial observations act as a control group in which mobility is at the baseline level (as individuals may not yet have voluntarily reduced their mobility as a response to reported cases). Furthermore, by ending at April 5, there can be no confounding of the effects of policy measures due to Easter holidays. Such confounding would be caused by that during holidays, mobility generally changes from regular levels and, as a consequence, policy measures are more or less likely to be implemented relative non-holidays.

Let  $M_{itk}$  denote the trip count on mobility variable  $k = 1, 2, \dots, K$  (i.e., total trips, road trips, train trips, etc.) in canton  $i = 1, 2, \dots, N$  on day  $t = 1, 2, \dots, T$ . The variable  $M_{itk}$  is derived as explained in the previous section and represents the dependent variable in regression model  $k$  for the DiD analysis. The values of the model parameters depend on which mobility variable is the dependent variable of the regression; hence, we index all model parameters with  $k$ .

We model  $M_{itk}$  to follow a negative binomial distribution with conditional mean function

$$\mathbb{E}[M_{itk} | \eta_{it}^{(k)}, E_i] = \mu(M_{itk}) = E_i \exp \eta_{it}^{(k)} \quad (1)$$

where  $E_i$  denotes the population size of canton  $i$ . Then,  $\exp \eta_{it}^{(k)} = (\mu(M_{itk}))/E_i$  is the expected number of daily trips per inhabitant in canton  $i$ . The estimates of this model are therefore adjusted according the variation in canton population sizes. The term  $\eta_{it}^{(k)}$  is the linear predictor, specified in hierarchical form as

$$\eta_{it}^{(k)} = \alpha_i^{(k)} + \delta_{w(t)}^{(k)} + \gamma^{(k)} \log z_{it} + \sum_{l=1}^L \beta_l^{(k)} d_{itl}, \quad (2)$$

$$\alpha_i^{(k)} = \alpha^{(k)} + \theta_i^{(k)} + \gamma_B^{(k)} \overline{\log z_i}, \quad (3)$$

whose variables and parameters are explained in the following.

The first term  $\alpha_i^{(k)}$  is a time-invariant effect specific to canton  $i$ . We model  $\alpha_i^{(k)}$  as a function of several variables that vary across cantons; see Equation (3). Here,  $\alpha^{(k)}$  is the intercept among all cantons, which represents the overall baseline relative mobility on Mondays before any policy measure was implemented and any COVID-19 cases were reported. The term  $\theta_i^{(k)}$  is a random effect that captures unobserved time-invariant factors for canton  $i$  (e.g., population density) that confound the effect of policy measures on mobility. The final variable  $\overline{\log z_i}$  is discussed in detail below. The subscript  $B$  on the associated parameter denotes that it measures between-canton effects; that is, the parameter only measures the effect of increases in the variable across cantons.

The variable  $d_{itl}$  is a dummy variable that takes a value of 1 if policy measure  $l \in \{1, 2, \dots, L\}$  is implemented by canton  $i$  at day  $t$  and 0 otherwise. Hence,  $\exp(\beta_l^{(k)})$  measures the multiplicative effect of policy measure  $l$  on the expected number of daily trips on mobility variable  $k$  per canton inhabitant. Note that all policy measure variables are included in (2). Hence, the effect of each policy measure is conditional on the other policy measures being held fixed. Figure 1c shows that

the reduction in mobility is similar across cantons; therefore, we do not estimate the heterogeneity in the effect of the policy measures on mobility across cantons.

The term  $\delta_{w(t)}^{(k)}$  represents the fixed effect of weekday  $w$  on the relative (log-transformed) mobility compared to the reference weekday (here: Monday). The term controls for the confounding factor that aggregate mobility and the probability of implementing a policy measure is likely higher on, e. g., Mondays than Sundays.

The variable  $z_{it}$  captures other sources of time-related confounding and is derived as follows. Let  $q_{it}$  be the number of days since the first reported COVID-19 case in canton  $i$ . The variable is calculated as

$$q_{it} = \begin{cases} t - t'_i, & \text{if } t > t'_i, \\ 0, & \text{if } t \leq t'_i, \end{cases} \quad (4)$$

where  $t'_i$  is the date the first case was reported in canton  $i$ . Since the logarithm of zero is undefined, we then set  $z_{it} = q_{it} + 1$  and include the logarithm of  $z_{it}$  in the model. The associated parameter  $\gamma^{(k)}$  is therefore interpreted as the percentage increase in relative mobility given a 1 % increase in the number of days since a canton first reported a case. The rationale for including  $z_{it}$  is that individuals may adapt their mobility behavior over time irrespective of social distancing policies. Therefore, the variable captures how mobility would trend over time even if the policy measures were not implemented.

The variable  $\bar{\log z_i} = T^{-1} \sum_{t=1}^T \log z_{it}$  is the time average of  $\log z_{it}$  in canton  $i$ . The bar over the expression denotes an average value. The variable is included in the model to allow the canton-specific effect  $\theta_i^{(k)}$  to be correlated with  $\log z_{it}$  over the cantons. Such correlation would, for instance, arise if the date that the first COVID-19 case is reported in each canton depends on the unobserved canton-specific factors. As an example, the date the first case is reported in a canton could depend on the (unobserved) adherence of inhabitants to social distancing recom-

mendations. If such correlation exists but is ignored, it would instead enter the error term of the model, leading to a violation of the exogeneity assumption and incorrect parameter estimates. By including  $\overline{\log z_i}$ , we essentially make  $\theta_i^{(k)}$  a Mundlak-type correlated random effect<sup>54</sup>. The benefit of correlated random effects over fixed effects or standard random effects is that they use only the within-unit variation to estimate parameters (and, hence, give identical estimates to those of fixed effects models) while also having the random effects property of estimating the variation in the unobserved heterogeneity via partial pooling. Note that time averages of the policy measure variables or weekday effects are not included in the model since those are exogenously determined and, therefore, uncorrelated with the model errors. We refer to<sup>55</sup> for a detailed discussion of the underlying benefits of this approach relative to fixed effects.

By substituting the linear predictor (2) into the conditional mean function (1) and expanding  $\alpha_i^{(k)}$ , the full model of mobility variable  $k$  becomes

$$\log \mathbb{E}[M_{itk} | \eta_{it}^{(k)}, E_i] = \log E_i + \alpha^{(k)} + \theta_i^{(k)} + \delta_{w(t)}^{(k)} + \gamma^{(k)} \log z_{it} + \gamma_B^{(k)} \overline{\log z_i} + \sum_{l=1}^L \beta_l^{(k)} d_{itl}. \quad (5)$$

The conditional variance of  $M_{itk}$  is given by

$$\mathbb{V}[M_{itk} | \eta_{it}^{(k)}, E_i, \zeta^{(k,M)}] = \mu(M_{itk}) \left( 1 + \frac{\mu(M_{itk})}{\zeta^{(k,M)}} \right), \quad (6)$$

where  $\zeta^{(k,M)}$  is the overdispersion parameter (the superscript  $M$  distinguishes the overdispersion parameter of the mobility model from the model of reported cases).

We specify one regression equation in the form of (5) for each mobility variable and estimate them separately. Each regression has the same explanatory variables but a different mobility variable as the dependent variable (i.e., total trips or one of the mobility variables based on mode or purpose).

## Model for estimating the relationship between mobility and COVID-19 cases

The model for estimating the relationship between mobility and reported COVID-19 cases is similar in structure to the model used to link policy measures to mobility. To accommodate the forecast horizon, we lag the mobility variables to estimate how a decrease in mobility at a given day predicts reductions on the reported number of new cases at a later day. This enables forecasting of future reported case growth by evaluating the model at daily observed mobility levels.

Let  $C_{it}$  denote the cumulative number of reported cases in canton  $i = 1, 2, \dots, N$  until and including day  $t = 1, 2, \dots, T_i$ . Then,  $Y_{it} = C_{it} - C_{i,t-1}$  is the number of new cases that are reported in canton  $i$  on day  $t$ . Note that the time frame (i.e., total number of days  $T_i$ ) varies across cantons  $i = 1, \dots, N$ . The reason for this is that the dependent variable of this regression model is the reported number of new cases, and as such we restrict the data to start at the date of each cantons first reported case. Hence, the data for this model starts between February 24 and March 16 (depending on the canton) and ends at April 5 (for all cantons). Our modeling approach accounts for the resulting unbalanced number of observations per canton.

We model  $Y_{it}$  as following a negative binomial distribution with a conditional mean function

$$\mathbb{E}[Y_{it} | \eta_{it}^{(k,s)}, E_i] = \mu^{(k,s)}(Y_{it}) = E_i \exp \eta_{it}^{(k,s)}, \quad (7)$$

where

$$\eta_{it}^{(k,s)} = \alpha_i^{(k,s)} + \delta_{w(t)}^{(k,s)} + \gamma^{(k,s)} \log z_{it} + \xi_{ks} \log m_{i,t-s,k}, \quad (8)$$

$$\alpha_i^{(k,s)} = \alpha^{(k,s)} + \theta_i^{(k,s)} + \gamma_B^{(k,s)} \overline{\log z_i} + \xi_{ks,B} \overline{\log m_{ik}} \quad (9)$$

is the hierarchical linear predictor. In this model,  $\exp \eta_{it}^{(k,s)} = (\mu^{(k,s)}(Y_{it}))/E_i$  is the expected number of reported positive cases in canton  $i$  on day  $t$  relative to the canton population size (sometimes called the relative risk in spatial epidemiological modeling<sup>56,57</sup>). The model for the daily growth

in reported cases can then be written as

$$\begin{aligned} \log \mathbb{E}[Y_{it} | \eta_{it}^{(k,s)}, E_i] &= \log E_i + \alpha^{(k,s)} + \theta_i^{(k,s)} + \delta_{w(t)}^{(k,s)} + \\ &\quad \gamma^{(k,s)} \log z_{it} + \gamma_B^{(k,s)} \overline{\log z_i} + \xi_{ks} \log m_{i,t-s,k} + \xi_{ks,B} \overline{\log m_{ik}}. \end{aligned} \quad (10)$$

The conditional variance of  $Y_{it}$  given mobility variable  $k$  lagged by  $s$  days is given by

$$\mathbb{V}[Y_{it} | \eta_{it}^{(k,s)}, E_i, \zeta^{(k,s,Y)}] = \mu^{(k,s)}(Y_{it}) \left( 1 + \frac{\mu^{(k,s)}(Y_{it})}{\zeta^{(k,s,Y)}} \right) \quad (11)$$

where  $\zeta^{(k,s,Y)}$  is the overdispersion parameter.

For simplicity, we use the same notation for variables and parameters in this model as in the model used for the effect of policy measures on mobility (but the estimated parameters have, of course, a different interpretation and values). The superscript  $(k, s)$  is attached to parameters to indicate that their values depend on the choice of mobility variable  $k$  and its lag  $s$ .

The parameter of interest is  $\xi_{ks}$ . It measures the expected percentage change in the reported number of new cases per canton inhabitant  $s$  days after a 1% increase in mobility variable  $k$ . Hence, the parameter shows how the relative growth rate in reported cases changes as a function of lagged mobility, after adjusting for relevant factors but where mobility varies according to which policy measures are implemented. Note that we intentionally include only a single lag  $s$  (and then refit the model for different lags) rather than including multiple lags at the same time. We follow this approach because infection disease dynamics imply that there are carry-on effects in infection rates between consecutive days that would be modeled as being fixed if several lags are included, resulting in biased estimates. We also only include only a single lagged mobility variable  $k$ . The reason is that every trip by mode or reason contributes to the total number of trips; hence, to avoid counting single trips several times, both the variable for the total number of trips and any variable for trips by mode or reason should not be included in the same model. Moreover, since

trips by mode or purpose are different subsets of total trips, every trip by one mode must be a trip of one purpose (e. g., a train trip is either made for the purpose of commuting or non-commuting); hence, for the same reason, the model should not include mobility variables for both a mode and a purpose. Supplement B.2 further explains our rationale.

The intercept  $\alpha^{(k,s)}$  gives the baseline number of reported cases relative to the canton population for Mondays.

The parameter  $\delta_{w(t)}^{(k,s)}$  is the effect of weekday  $w$  relative to the Monday effect. By including weekday effects in the model, we control for confounding differences in the number of trips and the number of reported COVID-19 cases between weekdays that would bias the parameter estimate on the lagged mobility variable. For instance, people travel to schools and work primarily on weekdays and, similarly, there are fewer COVID-19 tests on weekends and thus fewer reported cases on Monday/Tuesday (due to reporting delays).

The variable  $\log z_{it}$  is also included in this model. It now controls for the fact that mobility and the reported case growth both depend on when the first case was reported in a canton.

The Mundlak-style random effects  $\theta_i^{(k,s)}$  estimate the impact of unobserved canton-specific factors that may be correlated with both the variation in mobility across cantons and the logarithm of the number of days since the first case was reported in each canton. We achieve this by including variables of the time averages of  $\log z_{it}$  and lagged mobility, that is,  $\overline{\log m_{ik}} = T^{-1} \sum_{t-s} \log m_{i,t-s,k}$ . Then, any potential cross-canton correlation between the random effect and  $\log m_{i,t-s,k}$  or  $\log z_{it}$  via the models error term is controlled for.

The above regression model is fitted separately for each  $(k, s)$ , that is, each pair of mobility variable and lag. This allows us to investigate to what extent different lags of each mobility variable predict the number of reported cases.

## Estimation details

We estimate our models in a fully Bayesian framework. We run 4 Markov chains for every model, each with 2000 warm-up samples and another 2000 samples from the posterior distributions. Since our models are fitted with a log-link, we transform the posterior parameter samples so that they give estimates for the original scale of the dependent variable. For each parameter, we report in our plots the posterior mean and the associated 80 % and 95 % credible intervals (CrI) of the transformed posterior distribution.

The software used for estimation is the R package `brms`<sup>58,59</sup> version 2.11.1 built upon the statistical modeling platform Stan<sup>60</sup>. Parameter estimates are obtained by Markov chain Monte Carlo sampling in Stan version 2.19.2 using the Hamiltonian Monte Carlo algorithm<sup>61,62</sup> and the No-U-Turn sampler (NUTS)<sup>63</sup>.

Table 1 presents our choices of priors for the variables in the models. We use weakly informative priors to stabilize the computations and provide some regularization. Our prior on each  $\beta_l$  reflects that we expect each policy measure to reduce the logarithm of expected mobility with 25 %, on average, but that effects between 0–50 % are relatively probable. The prior on each  $\xi_{ks}$  implies that we expect that a 1 % decrease in the lagged mobility variable predicts a 1 % decrease in reported cases for each of the considered lags, with negative effect sizes or effect sizes exceeding 2 % being unlikely. The prior on  $\gamma$  implies that we expect the relative outcome to increase with 1 % for each 1 % increase in the number of days since the first reported case. The intercept, overdispersion parameter, and standard deviation of the canton random effects are given weakly informative priors. The prior on  $\delta_{w(t)}$  states that the effect of a given weekday that is not Monday should fall within 50–150 % of the Monday effect. The parameters for the variables of between-canton averages are assigned vague priors since we have no a priori belief of their effects.

Parameter	Description	Prior	Model
$\beta_l$	Policy measure $l$	$N(-0.25, 0.25)$	(5)
$\xi_{ks}$	Log mobility variable $k$ with a lag of $s$	$N(1, 1)$	(10)
$\alpha$	Intercept	Half-t(3, 1.8, 2.5)	(5), (10)
$\theta_i$	Canton random effect	$N(0, \sigma_\theta)$	(5), (10)
$\sigma_\theta$	Standard deviation for canton random effect	Half-t(3, 0, 2.5)	(5), (10)
$\delta_{w(t)}$	Weekday $w$ (compared to Monday)	$N(0, 0.5)$	(5), (10)
$\gamma$	Log no. of days since 1st reported case	$N(1, 1)$	(5), (10)
$\gamma_B$	Between-canton average of log no. of days since 1st reported case	$N(0, 5)$	(5), (10)
$\xi_{ks,B}$	Between-canton average of log mobility with a lag of $s$	$N(0, 5)$	(10)
$\zeta$	Overdispersion in dependent variable	Gamma(0.01, 0.01)	(5), (10)

*Note:* The superscripts  $(k)$  and  $(k, s)$  are omitted as the same priors are assigned to each model. The column “Description” states what effect the associated parameter represent (except for the overdispersion parameter).

Table 1: Choice of priors

## Model diagnostics

We followed common practice for model diagnostics of Bayesian models<sup>64</sup>. For each of the models, we inspected (1) posterior predictive checks, (2) divergent transitions, (3) effective sample size and convergence of the Markov chains, (4) overdispersion in the dependent variables, (5) influential observations, and (6) correlation between the policy parameters. All model diagnostics indicate a good fit. Details are provided in Supplement C.

## Robustness checks

First, we checked the robustness of the model estimates against alternative specifications of time effects: (a) A model specified as in the main paper but where the logarithmic trend is replaced with corresponding linear and quadratic trends (of the number of days since the first reported case

in each canton) to capture nonlinearities in both the reported case dynamics and general behavior towards social distancing. (b) A model with additional week fixed effects (i. e., a weekday fixed effect, a week fixed effect, and a trend variable in logarithmic form). This model allows us to control for weekly exogenous shocks (e. g., media reports about the shortage of critical care in Italy) but acknowledge that such fixed effects would be unknown at the time of forecasting and, therefore, cannot be used to predict reported case growth at a future date. All models yield similar estimates and hence confirm the explanatory power of the mobility variables (see Appendix [D.1](#)).

Second, the number of reported cases could potentially depend on the number of conducted tests per canton and day. When controlling for this, we obtain similar estimates (Appendix [D.2](#)).

Third, we extend the models by including a spatial random effect, as commonly used in the spatial epidemiology and disease mapping literature<sup>[65,66](#)</sup>. This approach allows us to account for the spatial dependence in mobility between neighbouring cantons. We find that the spatial dependence is low and retrieve estimated effects of policy measures that are practically identical to those of the main analysis (see Appendix [E.1](#)).

Fourth, we account for a potential dependence between different mobility variables and thus develop an estimation procedure for fitting their models jointly (that is, by modeling the covariance of the canton random effects for the different mobility variables). This model yields slightly narrower credible intervals but almost identical point estimates for the effects of the policy measures (see Appendix [E.2](#)).

## References

<sup>1</sup> World Health Organisation coronavirus disease (COVID-19) situation report. URL: <https://www.who.int/emergencies/diseases/novel-coronavirus-2019/situation-reports> (2020).

<sup>2</sup> Flaxman, S. *et al.* Estimating the effects of non-pharmaceutical interventions on COVID-19 in Europe. *Nature* **584**, 257–261 (2020).

<sup>3</sup> Hsiang, S. *et al.* The effect of large-scale anti-contagion policies on the COVID-19 pandemic. *Nature* **584**, 262–267 (2020).

<sup>4</sup> Ruktanonchai, N. W. *et al.* Assessing the impact of coordinated COVID-19 exit strategies across Europe. *Science* (2020).

<sup>5</sup> Lai, S. *et al.* Effect of non-pharmaceutical interventions to contain COVID-19 in China (2020).

<sup>6</sup> Unwin, H. J. T. *et al.* State-level tracking of COVID-19 in the united states. *Nature Communications* **11**, Article 6189 (2020).

<sup>7</sup> Grantz, K. H. *et al.* The use of mobile phone data to inform analysis of COVID-19 pandemic epidemiology. *Nature Communications* Article 4961 (2020).

<sup>8</sup> Benzell, S. G., Collis, A. & Nicolaides, C. Rationing social contact during the COVID-19 pandemic: Transmission risk and social benefits of US locations. *Proceedings of the National Academy of Sciences* (2020).

<sup>9</sup> Gao, S. *et al.* Mobile phone location data reveal the effect and geographic variation of social distancing on the spread of the COVID-19 epidemic. *arXiv* (2020).

<sup>10</sup> Chang, S. *et al.* Mobility network models of covid-19 explain inequities and inform reopening. *Nature* (2020).

<sup>11</sup> Dave, D. M., Friedson, A. I., Matsuzawa, K. & Sabia, J. J. When do shelter-in-place orders fight COVID-19 best? Policy heterogeneity across states and adoption time. *National Bureau of Economic Research* (2020).

<sup>12</sup> Gupta, S. *et al.* Tracking public and private response to the COVID-19 epidemic: Evidence from state and local government actions. *National Bureau of Economic Research* (2020).

<sup>13</sup> Adiga, A. *et al.* Interplay of global multi-scale human mobility, social distancing, government interventions, and COVID-19 dynamics. *medRxiv* (2020).

<sup>14</sup> Chinazzi, M. *et al.* The effect of travel restrictions on the spread of the 2019 novel coronavirus (COVID-19) outbreak. *Science* **368**, 395–400 (2020).

<sup>15</sup> Galeazzi, A. *et al.* Human mobility in response to COVID-19 in France, Italy and UK. *arXiv* (2020).

<sup>16</sup> Fang, H., Wang, L. & Yang, Y. Human mobility restrictions and the spread of the novel coronavirus (2019-nCoV) in China. *National Bureau of Economic Research* (2020).

<sup>17</sup> Kraemer, M. U. *et al.* The effect of human mobility and control measures on the COVID-19 epidemic in China. *Science* **368**, 493–497 (2020).

<sup>18</sup> Li, R. *et al.* Substantial undocumented infection facilitates the rapid dissemination of novel coronavirus (SARS-CoV-2). *Science* **368**, 489–493 (2020).

<sup>19</sup> Tian, H. *et al.* An investigation of transmission control measures during the first 50 days of the COVID-19 epidemic in China. *Science* **368**, 638–642 (2020).

<sup>20</sup> Bonaccorsi, G. *et al.* Economic and social consequences of human mobility restrictions under COVID-19. *Proceedings of the National Academy of Sciences* **117**, 15530–15535 (2020).

<sup>21</sup> Nouvellet, P. *et al.* Imperial College London COVID-19 response team – Report 26: Reduction in mobility and COVID-19 transmission (2020).

<sup>22</sup> Kang, Y. *et al.* Multiscale dynamic human mobility flow dataset in the US during the COVID-19 epidemic. *arXiv* (2020).

<sup>23</sup> Kogan, N. E. *et al.* An early warning approach to monitor COVID-19 activity with multiple digital traces in near real-time. *arXiv* (2020).

<sup>24</sup> Huang, J. *et al.* Understanding the impact of the COVID-19 pandemic on transportation-related behaviors with human mobility data. Proceedings of the 26th ACM SIGKDD International Conference on Knowledge Discovery & Data Mining (2020).

<sup>25</sup> Xiong, C., Hu, S., Yang, M., Luo, W. & Zhang, L. Mobile device data reveal the dynamics in a positive relationship between human mobility and COVID-19 infections. *Proceedings of the National Academy of Sciences* **117**, 27087–27089 (2020).

<sup>26</sup> Badr, H. S. *et al.* Association between mobility patterns and COVID-19 transmission in the USA: A mathematical modelling study. *The Lancet Infectious Diseases* (2020).

<sup>27</sup> Jia, J. S. *et al.* Population flow drives spatio-temporal distribution of COVID-19 in China. *Nature* 1–5 (2020).

<sup>28</sup> Jeffrey, B. *et al.* Imperial College London COVID-19 response team – Report 24: Anonymised and aggregated crowd level mobility data from mobile phones suggests that initial compliance with COVID-19 social distancing interventions was high and geographically consistent across the UK (2020).

<sup>29</sup> Pullano, G., Valdano, E., Scarpa, N., Rubrichi, S. & Colizza, V. Population mobility reductions during COVID-19 epidemic in France under lockdown. *medRxiv* (2020).

<sup>30</sup> Vinceti, M., Filippini, T., Rothman, K. J., Ferrari, F. & Goffi, A. Lockdown timing and efficacy in controlling COVID-19 using mobile phone tracking. *EClinicalMedicine*.

<sup>31</sup> Ruktanonchai, N. W. *et al.* Identifying malaria transmission foci for elimination using human mobility data. *PLOS Computational Biology* **12** (2016).

<sup>32</sup> Wesolowski, A. *et al.* Quantifying the impact of human mobility on malaria. *Science* **338**, 267–270 (2012).

<sup>33</sup> Viboud, C. & Vespignani, A. The future of influenza forecasts. *Proceedings of the National Academy of Sciences* **116**, 2802–2804 (2019).

<sup>34</sup> Bengtsson, L. *et al.* Using mobile phone data to predict the spatial spread of cholera. *Scientific Reports* **5**, 8923 (2015).

<sup>35</sup> Wesolowski, A. *et al.* Quantifying seasonal population fluxes driving rubella transmission dynamics using mobile phone data. *Proceedings of the National Academy of Sciences* **112**, 11114–11119 (2015).

<sup>36</sup> Wesolowski, A. *et al.* Impact of human mobility on the emergence of dengue epidemics in Pakistan. *Proceedings of the National Academy of Sciences* **112**, 11887–11892 (2015).

<sup>37</sup> Reuters. European mobile operators share data for coronavirus fight. URL: <https://www.reuters.com/article/us-health-coronavirus-europe-telecoms-idUSKBN2152C2> (2020).

<sup>38</sup> Buckee, C. O. *et al.* Aggregated mobility data could help fight COVID-19. *Science* **368**, 145 (2020).

<sup>39</sup> Kishore, N. *et al.* Measuring mobility to monitor travel and physical distancing interventions: A common framework for mobile phone data analysis. *The Lancet Digital Health* (2020).

<sup>40</sup> Desai, A. N. *et al.* Real-time epidemic forecasting: Challenges and opportunities. *Health Security* **17**, 268–275 (2019).

<sup>41</sup> Blumenstock, J., Cadamuro, G. & On, R. Predicting poverty and wealth from mobile phone metadata. *Science* **350**, 1073–1076 (2015).

<sup>42</sup> Bertozzi, A. L., Franco, E., Mohler, G., Short, M. B. & Sledge, D. The challenges of modeling and forecasting the spread of COVID-19. *Proceedings of the National Academy of Sciences* **117**, 16732–16738 (2020).

<sup>43</sup> Oliver, N. *et al.* Mobile phone data for informing public health actions across the COVID-19 pandemic life cycle. *Science Advances* **6**, eabc0764 (2020).

<sup>44</sup> Swisscom. Swisscom Mobility Insights. URL: <https://www.swisscom.ch/en/business/enterprise/offer/enterprise-mobile/mobility-insights.html> (2020).

<sup>45</sup> Kraemer, M. U. *et al.* Mapping global variation in human mobility. *Nature Human Behaviour* **4**, 800–810 (2020).

<sup>46</sup> Standorte Mobilfunkmasten GSM. URL: <https://opendata.swisscom.com/explore/dataset/standorte-mobilfunkmasten-gsm/table/?disjunctive.powercode&sort=-id> (2020).

<sup>47</sup> Standorte Mobilfunkmasten UMTS. URL: [https://opendata.swisscom.com/explore/dataset/xy\\_pwr\\_umts\\_170101/information/?disjunctive.powercode](https://opendata.swisscom.com/explore/dataset/xy_pwr_umts_170101/information/?disjunctive.powercode) (2020).

<sup>48</sup> Standorte Mobilfunkmasten LTE. URL: <https://opendata.swisscom.com/explore/dataset/standorte-mobilfunkmasten-lte/information/?disjunctive.powercode> (2020).

<sup>49</sup> Kafsi, M. Quantifying the accuracy of mobility insights from cellular network data. URL: <https://mkafsi.medium.com/quantifying-the-accuracy-of-mobility-insights-from-cellular-network-data-e> (2019).

<sup>50</sup> Leontiadis, I. *et al.* From cells to streets: Estimating mobile paths with cellular-side data. *ACM International on Conference on Emerging Networking Experiments and Technologies* (2014).

<sup>51</sup> Bassolas, A. *et al.* Hierarchical organization of urban mobility and its connection with city livability. *Nature Communications* **10**, 1–10 (2019).

<sup>52</sup> Gonzalez, M. C., Hidalgo, C. A. & Barabasi, A.-L. Understanding individual human mobility patterns. *Nature* **453**, 779–782 (2008).

<sup>53</sup> Goodman-Bacon, A. Difference-in-differences with variation in treatment timing. *National Bureau of Economic Research* (2018).

<sup>54</sup> Mundlak, Y. On the pooling of time series and cross section data. *Econometrica: Journal of the Econometric Society* **46**, 69–85 (1978).

<sup>55</sup> Bell, A. & Jones, K. Explaining fixed effects: Random effects modeling of time-series cross-sectional and panel data. *Political Science Research and Methods* **3**, 133–153 (2015).

<sup>56</sup> Riebler, A., Sørbye, S. H., Simpson, D. & Rue, H. An intuitive Bayesian spatial model for disease mapping that accounts for scaling. *Statistical Methods in Medical Research* **25**, 1145–1165 (2016).

<sup>57</sup> Asmari, N., Ayatollahi, S. M. T., Sharifi, Z. & Zare, N. Bayesian spatial joint model for disease mapping of zero-inflated data with R-INLA: A simulation study and an application to male breast cancer in Iran. *International Journal of Environmental Research and Public Health* **16**, 4460 (2019).

<sup>58</sup> Bürkner, P. C. BRMS: An R package for Bayesian multilevel models using Stan. *Journal of Statistical Software* **80**, 1–28 (2017).

<sup>59</sup> Bürkner, P. C. Advanced Bayesian multilevel modeling with the R Package BRMS. *The R Journal* **10**, 395–411 (2018).

<sup>60</sup> Carpenter, B. *et al.* Stan: A probabilistic programming language. *Journal of Statistical Software* **76** (2017).

<sup>61</sup> Neal, R. M. *et al.* MCMC using Hamiltonian dynamics. *Handbook of Markov Chain Monte Carlo* **2**, 2 (2011).

<sup>62</sup> Duane, S., Kennedy, A. D., Pendleton, B. J. & Roweth, D. Hybrid Monte Carlo. *Physics Letters B* **195**, 216–222 (1987).

<sup>63</sup> Hoffman, M. D. & Gelman, A. The No-U-Turn sampler: Adaptively setting path lengths in Hamiltonian Monte Carlo. *Journal of Machine Learning Research* **15**, 1593–1623 (2014).

<sup>64</sup> Gelman, A. *et al.* *Bayesian Data Analysis* (CRC press, 2013).

<sup>65</sup> Besag, J., York, J. & Mollié, A. Bayesian image restoration, with two applications in spatial statistics. *Annals of the Institute of Statistical Mathematics* **43**, 1–20 (1991).

<sup>66</sup> Wakefield, J., Best, N. & Waller, L. Bayesian approaches to disease mapping. *Spatial Epidemiology: Methods and Applications* 104–127 (2000).

<sup>67</sup> Cheng, C., Barceló, J., Hartnett, A. S., Kubinec, R. & Messerschmidt, L. COVID-19 government response event dataset (CoronaNet v. 1.0). *Nature Human Behaviour* **4**, 756–768 (2020).

<sup>68</sup> Hale, T., Petherick, A., Phillips, T. & Webster, S. Univeristy of Oxford Blavatnik school of Government – Variation in government responses to COVID-19 (2020).

<sup>69</sup> Rubin, D. B. Estimating causal effects of treatments in randomized and nonrandomized studies. *Journal of Educational Psychology* **66**, 688 (1974).

<sup>70</sup> Holland, P. W. Statistics and causal inference. *Journal of the American Statistical Association* **81**, 945–960 (1986).

<sup>71</sup> Lauer, S. A. *et al.* The incubation period of coronavirus disease 2019 (COVID-19) From publicly reported confirmed cases: Estimation and application. *Annals of Internal Medicine* **172**, 577–582 (2020).

<sup>72</sup> Vehtari, A. *et al.* Efficient leave-one-out cross-validation and WAIC for Bayesian models (2020). URL <https://mc-stan.org/loo>. R package version 2.3.1.

<sup>73</sup> Gabry, J. & Mahr, T. Bayesplot: Plotting for Bayesian models (2020). URL <https://mc-stan.org/bayesplot>. R package version 1.7.2.

<sup>74</sup> Gabry, J., Simpson, D., Vehtari, A., Betancourt, M. & Gelman, A. Visualization in Bayesian workflow. *Journal of the Royal Statistical Society: Series A (Statistics in Society)* **182**, 389–402 (2019).

<sup>75</sup> Vehtari, A., Gelman, A. & Gabry, J. Practical Bayesian model evaluation using leave-one-out cross-validation and WAIC. *Statistics and computing* **27**, 1413–1432 (2017).

<sup>76</sup> Vehtari, A., Simpson, D., Gelman, A., Yao, Y. & Gabry, J. Pareto smoothed importance sampling. *arXiv preprint arXiv:1507.02646* (2015).

<sup>77</sup> Morris, M. Spatial models in Stan: Intrinsic auto-regressive models for areal data. URL: [https://mc-stan.org/users/documentation/case-studies/icar\\_stan.html](https://mc-stan.org/users/documentation/case-studies/icar_stan.html) (2019).

<sup>78</sup> Morris, M. *et al.* Bayesian hierarchical spatial models: Implementing the Besag York Mollié model in Stan. *Spatial and Spatio-Temporal Epidemiology* **31**, 100301 (2019).

<sup>79</sup> Simpson, D. *et al.* Penalising model component complexity: A principled, practical approach to constructing priors. *Statistical Science* **32**, 1–28 (2017).

<sup>80</sup> Dean, C., Ugarte, M. & Militino, A. Detecting interaction between random region and fixed age effects in disease mapping. *Biometrics* **57**, 197–202 (2001).

<sup>81</sup> Zellner, A. An efficient method of estimating seemingly unrelated regressions and tests for aggregation bias. *Journal of the American Statistical Association* **57**, 348–368 (1962).

<sup>82</sup> Baron, R. M. & Kenny, D. A. The moderator–mediator variable distinction in social psychological research: Conceptual, strategic, and statistical considerations. *Journal of Personality and Social Psychology* **51**, 1173 (1986).

<sup>83</sup> Yuan, Y. & MacKinnon, D. P. Bayesian Mediation Analysis. *Psychological Methods* **14**, 301 (2009).

<sup>84</sup> Imai, K., Keele, L. & Tingley, D. A General Approach to Causal Mediation Analysis. *Psychological Methods* **15**, 309 (2010).

<sup>85</sup> Imai, K., Keele, L. & Yamamoto, T. Identification, Inference and Sensitivity Analysis for Causal Mediation Effects. *Statistical Science* 51–71 (2010).

<sup>86</sup> Gelman, A. *et al.* Prior distributions for variance parameters in hierarchical models (comment on article by Browne and Draper). *Bayesian Analysis* **1**, 515–534 (2006).

## Data availability

Human mobility data presented in this work are available from the Swisscom Mobility Insights Platform (<https://mip.swisscom.ch>). Cantonal geographic boundaries can be found as shape files at the official portal of the Swiss government (<https://shop.swisstopo.admin.ch/en/products/landscape/boundaries3D>).

Data on cumulative reported COVID-19 cases per canton and relative to the cantonal population size (i.e., cases per 100,000 inhabitants) come from the Federal Office of Public Health of the Swiss Confederation; BAG (<https://covid-19-schweiz.bagapps.ch/de-1.html>). We also use this source to obtain data on the total number of daily tests conducted in Switzerland. Additional information on the Swiss population come from the Swiss Federal Statistical Office; BFS (<https://www.bfs.admin.ch/bfs/en/home/statistics/population.html>). Data on the population size per Swiss canton are obtained from the Swiss Federal Statistical Office (<https://www.bfs.admin.ch/asset/en/1155-1800>). We use the 2018 permanent resident population statistics by canton as these are the most recently published official numbers. Details on policy measure data collection are provided in Appendix A. When referring to cantons, we use abbreviations instead of full canton names (<https://www.admin.ch/ch/d/gg/pc/documents/1336/Abkuerzungsverzeichnis.pdf>).

## Ethics declarations

**Competing interests.** S.F. declares membership in a *COVID-19 Working Group* by the *World Health Organization* (WHO) but without competing interests. Furthermore, S.F. acknowledges funding from the *Swiss National Science Foundation* (SNSF) on data-driven health management, yet outside of the submitted work. The funding bodies had no control over design, conduct, data, analysis, review, reporting, or interpretation of the research conducted.

**Ethics approval.** Ethics approval (2020-N-41) was obtained from the institutional review board at ETH Zurich.

**Author contributions.** J.P. and S.F. contributed to conceptualization, data collection, data analysis (modeling), results interpretation, and manuscript writing. J.F.P. contributed to conceptualization, data collection, data analysis (exploratory), results interpretation, and manuscript writing.

**Acknowledgments.** We thank Dominik Hangartner and Achim Ahrens for the invaluable feedback. We also thank Swisscom for their extensive support.

**Correspondence.** Joel Persson ([jpersson@ethz.ch](mailto:jpersson@ethz.ch))

# Supplements

## A Data

### A.1 Policy measures

We collected data on policy measures implemented at both national level directly from the official resources of the federal government in Switzerland ([www.admin.ch](http://www.admin.ch)). Implementations of policy measures at sub-national (cantonal) level were collected from official resources of the cantonal authorities (e. g., [www4.ti.ch](http://www4.ti.ch), [www.ge.ch](http://www.ge.ch)). These policy measures were implemented throughout the complete canton (i. e., there is no “partial” implementation). We then checked our data on policy measures against benchmark datasets, namely the government response event dataset CoronaNet<sup>67</sup>, the Government Response Tracker<sup>68</sup> and the Swiss National COVID-19 Science Task Force (<https://ncs-tf.ch/en/situation-report>). As our goal is to study the response and impact of mobility, we excluded policy measures that were primarily used to target physical distance and not mobility. Examples of such policy measures is the requirement to wear a mask or the recommendation to keep a physical distance of at least 1.5 meters between people.

The policy measures were encoded as follows. We encoded “school closures” such that the closure falls on a weekday. That is, when school closures were put into effect on a Saturday, we encoded “school closures” as being closed from Monday onwards. The reason is that both primary and secondary schools are, by default, closed on weekends and, hence, movements from/to school can only be in effect on the next weekday. Different from other countries, schools were closed not “partially”, e. g., for specific age groups, but for all. We encoded “closed border” such that this policy measure is in effect when any side of the border is closed. As an example, when Italy closed its border, we encoded the borders for the adjacent cantons as closed. The rationale is that trips will

be cancelled if people cannot return. For all cantons without borders to other countries, we encoded “border closures” as implemented when the national government decided put travel restrictions in place. Consider Zurich as an example. The cantonal government of Zurich did not put travel restrictions into effect, and, hence, we set “border closures” for the canton of Zurich to March 25, 2020, which is the date when the national government enforced travel restrictions. Before that date, travel into the canton was possible through Zurich airport and it was only restricted from March 25, 2020 onward due to the national (and not the cantonal) government.

The resulting list of policy measures is shown in Table 2. All of these policy measures remained in effect from the day of their implementation until the end of our study period (i.e., through April 26, 2020). Furthermore, note the cross-canton variation in implementation dates for some of the policy measures. The difference in timing for a given policy measure is one of the aspects that enables us identify the effects of the policy measures with the difference-in-difference analysis. These comparisons better approximate differences between a treatment and control group when the cantons are comparable by having similar values on unobservable and included control variables in the regression model (see [Model for estimating the reduction in human mobility due to policy measures](#)). An example of a comparable difference is that between St. Gallen (SG) and Lucerne (LU). These cantons are similar in geographical size, population size, and population density, but whereas SG implemented border closures on March 14, LU was not affected by border closures until March 25 (Table 2). Hence, between these dates, LU provide control observations for SG that enable us to identify the effect of borders closures in the whole country.

Implementation date	Policy measure	Description	Cantons
10-03-2020	Border closures	Italian border closed	GR, TI, VS
13-03-2020	Ban > 100	Ban on gatherings with > 100 people	AG,AR,AI,BL,BS,BE,FR,GE,GL, GR,JU,LU,NE,NW,OW,SH,SZ,SO, SG,TI,TG,UR,VD,VS,ZG,ZH
14-03-2020	Venue closures	Closure of venues	TI
14-03-2020	Border closures	Austrian border closed	GR, SG
16-03-2020	School closures	Closure of primary and high schools	AG,AR,AI,BL,BS,BE,FR,GE,GL, GR,JU,LU,NE,NW,OW,SH,SZ,SO, SG,TI,TG,UR,VD,VS,ZG,ZH
17-03-2020	Venue closures	Closure of non-essential stores (all businesses except supermarkets, food suppliers and pharmacies), museums, zoos, hairdressers, garden centers, restaurants, night-clubs and bars	AG,AR,AI,BL,BS,BE,FR,GE,GL, GR,JU,LU,NE,NW,OW,SH,SZ,SO, SG,TI,TG,UR,VD,VS,ZG,ZH
17-03-2020	Border closures	German border closed	AG, BL, BS, SH, TG, ZH
18-03-2020	Ban > 5	Ban on gatherings with > 5 people	JU, VD
20-03-2020	Ban > 5	Ban on gatherings with > 5 people	AG,AR,AI,BL,BS,BE,FR,GE,GL, GR,JU,LU,NE,NW,OW,SH,SZ,SO, SG,TI,TG,UR,VD,VS,ZG,ZH
18-03-2020	Border closures	French border closed	GE, JU, NE, VD
25-03-2020	Border closures	Swiss border closed	AG,AR,AI,BL,BS,BE,FR,GE,GL, GR,JU,LU,NE,NW,OW,SH,SZ,SO, SG,TI,TG,UR,VD,VS,ZG,ZH

Table 2: Timeline of policy measure implementations across sub-national levels (cantons). When referring to cantons, we use abbreviations from <https://www.admin.ch/ch/d/gg/pc/documents/1336/Abkuerzungsverzeichnis.pdf>.

## A.2 Variation in timing of policy measures across cantons

We summarize the spatio-temporal heterogeneity across cantons of when policy measures were put into effect. For this, we first study the difference in days between cantons of when any pair of two policy measures were implemented. We take the absolute value of the difference in days as the difference should not depend on which canton implemented a policy measure first. We then calculate the mean and median of the absolute differences to obtain easily interpretable summary statistics of the variation in timing. Table 3 shows that the policy measures are rarely implemented close in time; instead, there is a substantial delay between implementation dates across cantons. This variation among policy measures between cantons enables us to disentangle the effects of the different policy measures and affects the precision of their estimated effects. See Appendix C.6 and Figure 18 for a further discussion.

	Ban > 100	School closures	Venue closures	Ban > 5	Border closures		Ban > 100	School closures	Venue closures	Ban > 5	Border closures	
Ban > 100	—	3.0	3.9	6.9	7.8		Ban > 100	—	3.0	4.0	7.0	5.0
School closures	3.0	—	1.0	3.9	5.6		School closures	3.0	—	1.0	4.0	6.0
Venue closures	3.9	1.0	—	3.0	4.8		Venue closures	4.0	1.0	—	3.0	7.0
Ban > 5	6.9	3.9	3.0	—	4.6		Ban > 5	7.0	4.0	3.0	—	5.0
Border closures	7.8	5.6	4.8	4.6	—		Border closures	5.0	6.0	7.0	5.0	—

Table 3: Variation in implementation dates of policy measures across cantons (absolute time difference in days): mean (left) and median (right).

## B Identification strategy

This section explains how the model estimates are identified from the data. In doing so we also explain the assumptions underlying the modeling.

### B.1 Estimating the reduction in human mobility due to policy measures through a difference-in-difference analysis

The parameter estimates for the policy measures can be interpreted as causal effects under the following standard assumptions for difference-in-difference (DiD) analysis: (1) the policy measures were implemented (a) “as if” independently of the level of mobility or, (b) in the absence of any policy measure, all cantons would have parallel trends in mobility; (2) the canton population distributions were stable over time; and (3) the implementation of each policy measure in any canton did not affect the mobility in any other canton.

Assumption (1a) implies that there are no omitted confounders of the relation between policy measures and mobility. This seems credible conditional on unobserved canton-specific and weekday-specific factors, the time since the a canton’s first reported case, and a canton’s population size. We therefore adjust for these factors in our model. Note that assumption 1a is stronger than assumption 1b but that both are sufficient for the causal interpretation together with assumption (2) and (3). Hence if assumption (1a) does not hold, the DiD estimates can still be interpreted as causal effects under assumptions (1b), (2), and (3) together. In our context, assumption 1b implies that, if no policy measures was implemented, mobility would trend (or not trend) in the same way for all cantons. Then for a given day, the cantons that have not yet implemented a policy measure provide valid control observations for the cantons that have implemented the policy measure. This assumption is inherently untestable, but likely holds since the cantons had parallel levels of mobility prior to the policy measures (see Fig. 1 in the main paper).

Assumptions (2) and (3) are together known as the stable unit treatment value assumption<sup>69,70</sup>,

which is a standard assumption in the causal inference literature and for difference-in-difference analysis. Assumption 2 seems plausible given the official recommendations to limit long-distance travel, the lockdown of many European countries at the time, and that our data cover close to the whole Swiss population. The credibility of Assumption (3) is debatable since some people may, for precautionary reasons, reduce their mobility when a policy measure that is not yet implemented in their canton is implemented in another canton. The assumption could be relaxed by estimating effects of the policy measures across cantons, but this would increase the modeling complexity substantially and lead to more difficult interpretation of the results. Note that even if the above assumptions for causality do not hold, the estimates from the DiD analysis are still useful as they then give the conditional association between mobility and policy measures.

The analysis also requires the variables to follow a specific measurement order in time. To measure the effect of policy measures on mobility within days, they must – for each day – be implemented earlier than mobility is measured. This holds true in our study. The policy measures were put into effect at midnight at their date of implementation in Switzerland, while movements were then collected for subsequent days. Recall that, for each mobility variable, we calculate the number of trips by aggregating the total number over the full day. Hence, the measurement order is such that the policy measures precede mobility.

Altogether, the above elaboration points to assumptions under which the estimations can be interpreted to be causal effects.

## B.2 Estimating how reductions in mobility predict COVID-19 cases

We estimate the conditional relationship between lagged mobility and the reported number of COVID-19 cases using a regression model. We control for variables that confound the relationship between mobility and reported cases but let the policy measures vary. The regression thereby identifies the extent to which the level of mobility at a given day predicts the number of new cases reported in a later day when both depend on policy measures. By lagging mobility, we rule out

the possibility that the parameter estimates for mobility are biased by simultaneity or reversed causality, meaning that there are feedback loops between mobility and reported cases or that the number of reported cases affect mobility.

Two factors determine the delay of mobility in predicting the reported number of new cases: (1) the incubation period, and (2) the reporting delay. Previously, the mean incubation period was estimated to 5.1 days, while 97.5 % of infected people had symptoms within 11.5 days after exposure<sup>71</sup>. Adding a 2 day reporting delay (cf. the case data from the Federal Office of Public Health of the Swiss Confederation; BAG) leads to the chosen lags of mobility of 7–13 days.

We fit the regression model separately for each lag and mobility variable. It would also be possible to fit the regression with all lags of one mobility variable included. However, this approach was discarded because of the following reason. Infection dynamics imply that the growth rate in reported cases at a given day depends on earlier growth rates. Hence, the relationship between mobility and the reported number of new cases at a given date is partially an outcome of their relationship at an earlier date. Including all lags of a mobility variable in the model would restrict this dependence. The parameter estimate associated with each lag of mobility would then reflect how mobility at a given day predicts the number of cases reported in the number of days ahead given by the lag, after the predicted change of the other lags of mobility has been removed. To address this concern, our model specification includes only a single lag.

For a similar reason as above, the regression model was specified to include only a single mobility variable (and not all mobility variables at the same time). Here the rationale is as follows. Trips by mode and purpose are different subsets of total trips. A trip of one purpose is therefore also a trip of one mode. For instance, every trip by train is either a commuter trip or non-commuter trip. Including all mobility variables in the same regression would artificially hold the variables in the subsets fixed against each other, resulting in incorrect estimates. This is ruled out in our model specification where a only single mobility variable is included but where the model is re-estimated for different ones.

## C Model diagnostics

This section presents an analysis of model diagnostics. For reasons of brevity, we only show diagnostics for the models with the total trips variable. The diagnostics for the models of trips by each mode and purpose also showed good fit.

The R package `loo`<sup>72</sup> version 2.3.1 is used to estimate the Pareto tail shape parameter and, based on it, check for influential observations. The other diagnostic plots are obtained with the R package `bayesplot`<sup>73,74</sup> version 1.7.2.

### C.1 Checking posterior predictive ability

We assess model fit through posterior predictive checks. For each model, we simulate 10 draws from its posterior predictive distributions with the same values of the explanatory variables as those used to fit the model, resulting in simulated replicates of the response variable. Consistent with the notation in<sup>64</sup> we denote these  $y_{rep}$ . Figure 6 and Figure 7 shows kernel density estimates of the replicated responses and the observed responses for the models of mobility and cases. The replicated response densities fit the observed response density well, indicating good model fit.

### C.2 Checking for divergent transitions

Figure 8 shows Kernel density and time series of the MCMC samples of the parameters for the mobility model. Figure 11 shows the autocorrelation among the MCMC samples of the same parameters. Figure 9 and Figure 11 shows the same information for the models with cases as dependent variables. For brevity we omit the corresponding plots for control variables, intercepts and random and fixed effects. For each lag of total trips, the posterior density of the parameter is approximately Gaussian and that their chains have good mixing with no signs of divergence or substantial autocorrelation.

### C.3 Checking the effective sample size and convergence of Markov chains

Figure 12 and Figure 14 shows ratios of effective sample size to total sample size ( $\hat{n}_{\text{eff}}/N$ ) and  $\hat{R}$  values, respectively, for the MCMC samples of all parameters in the regression models. The corresponding plots for the models of cases are available in Figure 13 and Figure 15. The ratio of effective sample size to total sample size is between around 0.4 and 1 for most parameters, indicating a sufficient number of independent draws from the posterior distributions<sup>64</sup>. The  $\hat{R}$  values are close to 1 for all parameters and models. Hence, this indicates convergence of the Markov chains.

### C.4 Checking for overdispersion

The estimated overdispersion parameter (for the models with total trips) is as follows:

- The first model (for estimating the reduction in human mobility due to policy measures) has an estimated overdispersion parameter of 51.33 (95 % CrI: 47.02–55.88).
- The second model (for estimating the relationship between mobility and cases) has an estimated overdispersion parameter of 3.43 (95 % CrI: 2.92–3.99) at a lag of 7 days. The parameter estimate amounts to 3.95 (95 % CrI: 3.34–4.65) at a lag of 13 days.
- In the mediation analysis, the estimated overdispersion parameter of the mediation model amounts to 54.40 (95 % CrI: 49.49–59.54) for a lag of 7 days. The estimate increases to 61.83 (95 % CrI: 56.14–67.71) for a lag of 13 days. For the outcome model, the estimated overdispersion parameter increases from 4.29 (95 % CrI: 3.60–5.06) at a lag 7 to an estimate of 5.42 (95 % CrI: 4.48–6.49) at lag 13.

Overall, there is substantial overdispersion in the dependent variables. Because this, the use of a negative binomial distribution for the dependent variables is recommended.

## C.5 Checking for influential observations

Influential observations can have a negative effect on model fit. To check for the presence of influential observations, we plot the Pareto tail shape parameter  $k$  against the observation indices for each of the models. The results for the model of total trips are shown in Figure 16 while the results for the model of cases on total trips are available in Figure 17. A value of  $k$  less than 0.5 is generally considered good whereas a value between 0.5–0.7 is considered okay<sup>75,76</sup>. No model has many observations with an estimated value of  $k$  above 0.5.

## C.6 Checking for correlations between parameters

A similar timing of the policy measures across cantons could make it difficult to distinguish their individual effects. To investigate this issue, Figure 18 depicts scatterplots of the pairwise bivariate posterior distributions of the policy measure parameters. There is a negative correlation between the posterior samples of the parameters for some of the NPI pairs, reflecting a difficulty to distinguish the effects of the two policy measures if they are introduced close in time. It seems to be somewhat difficult to distinguish between the effects of the ban on gatherings and school closures, as they were implemented close in time in many cantons (Table 3). The same holds for the bans of gatherings of more than five people and border closures. In contrast, the effects of border closures, school closures, and venue closures can be distinguished, as judged by the even spread of their pairwise scatters (Figure 18).

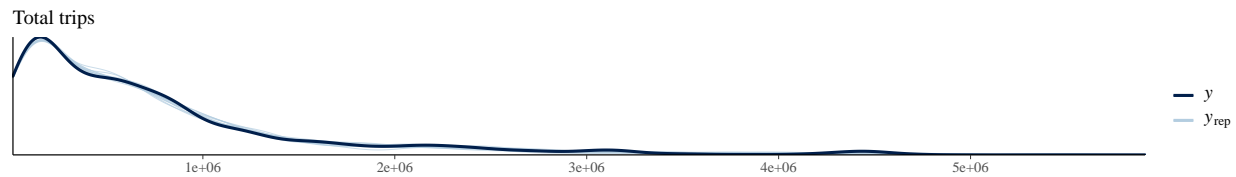


Figure 6: Posterior predictive plot for the model of the effect of the policy measures on total trips.  $y$  and  $y_{rep}$  are kernel density estimates of the observed response values and 10 simulated replicates, respectively.

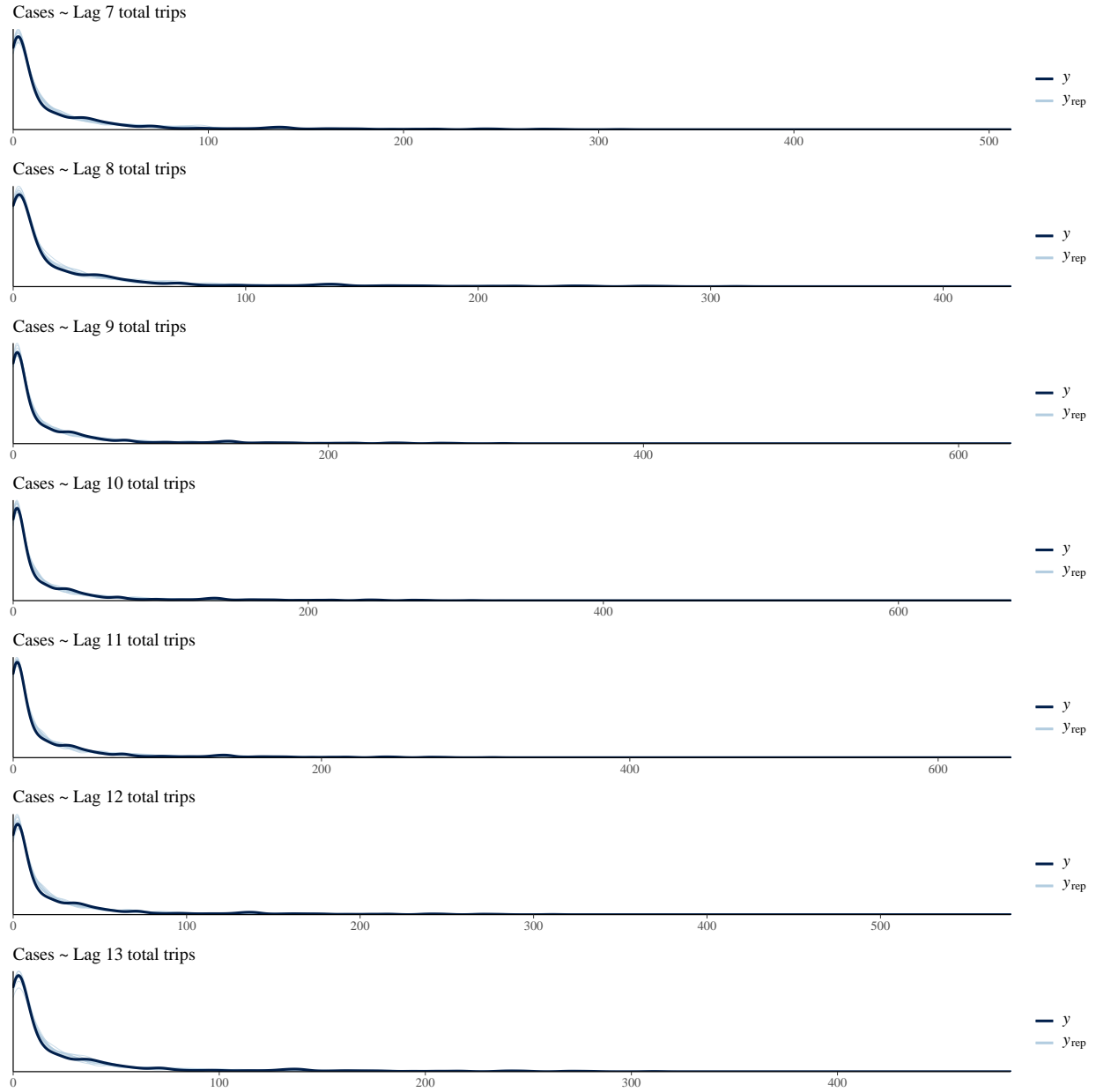


Figure 7: Posterior predictive plot of the model for the effect of each lag of total trips on the reported number of new cases.  $y$  and  $y_{rep}$  are kernel density estimates of the observed response values and 10 simulated replicates, respectively.

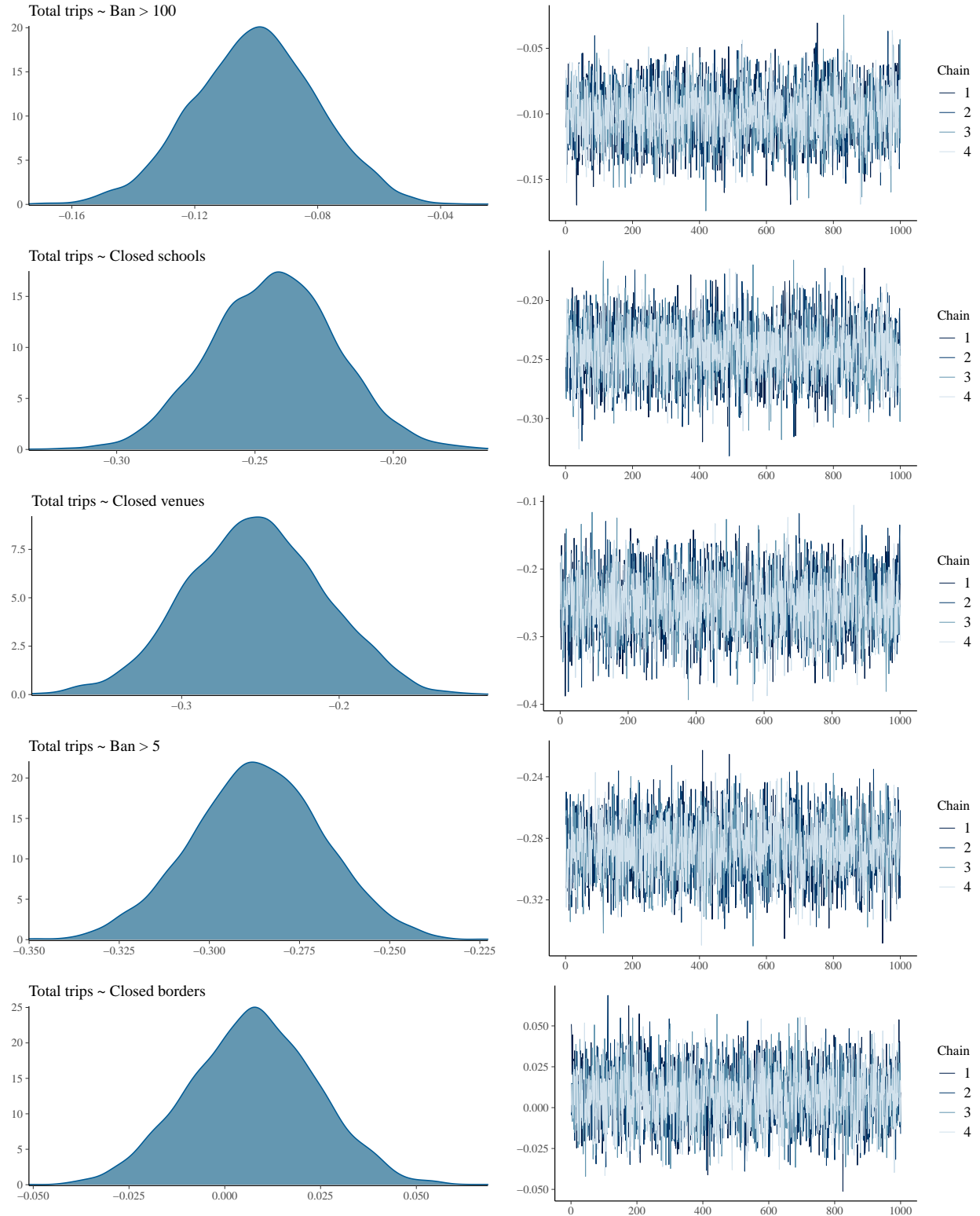


Figure 8: Kernel density and time series plots of the MCMC samples of the parameter for the effect of each policy measure and total trips.

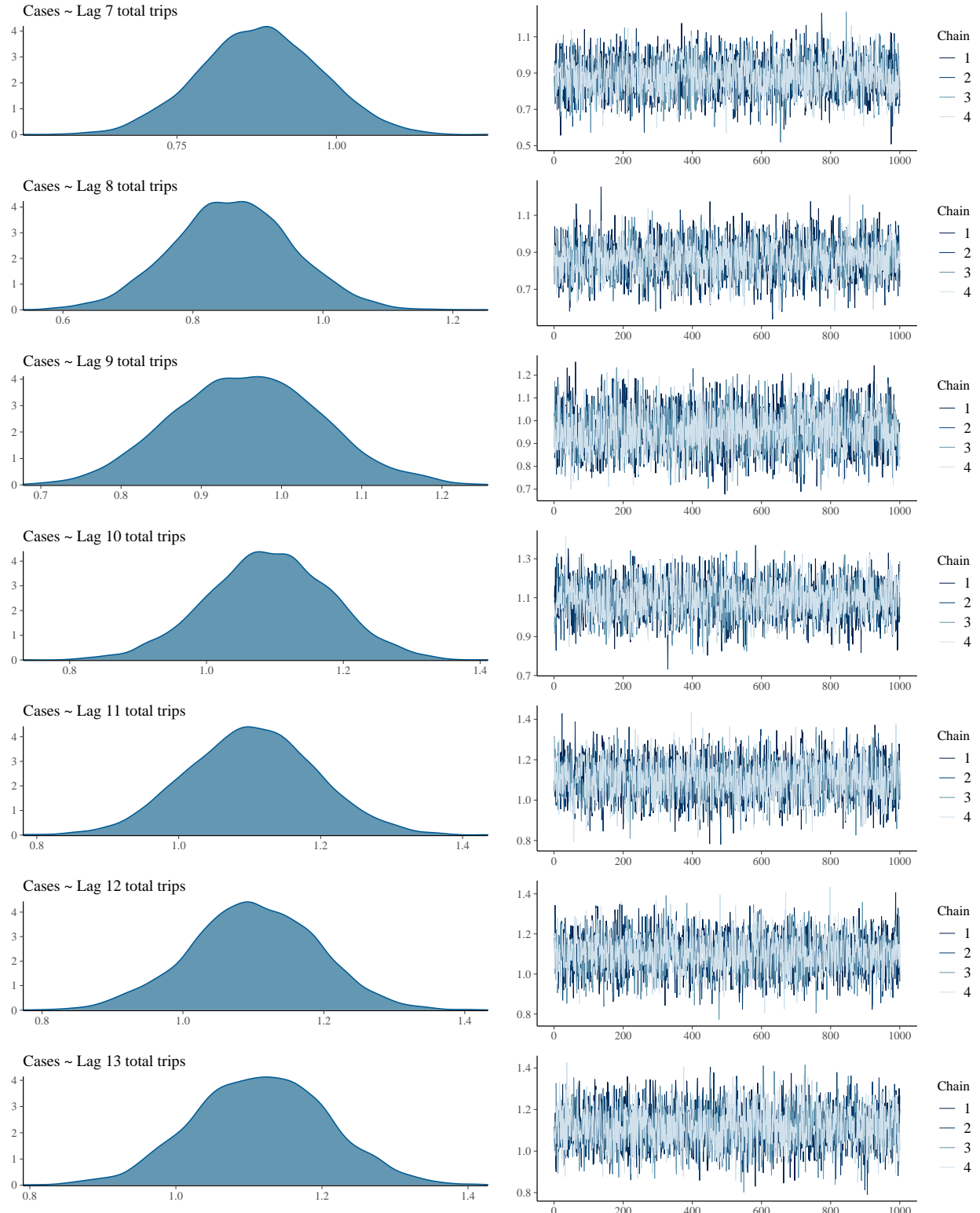


Figure 9: Kernel density and time series plots of the MCMC samples of the parameter for the effect of each lag of total trips on the reported number of new cases.

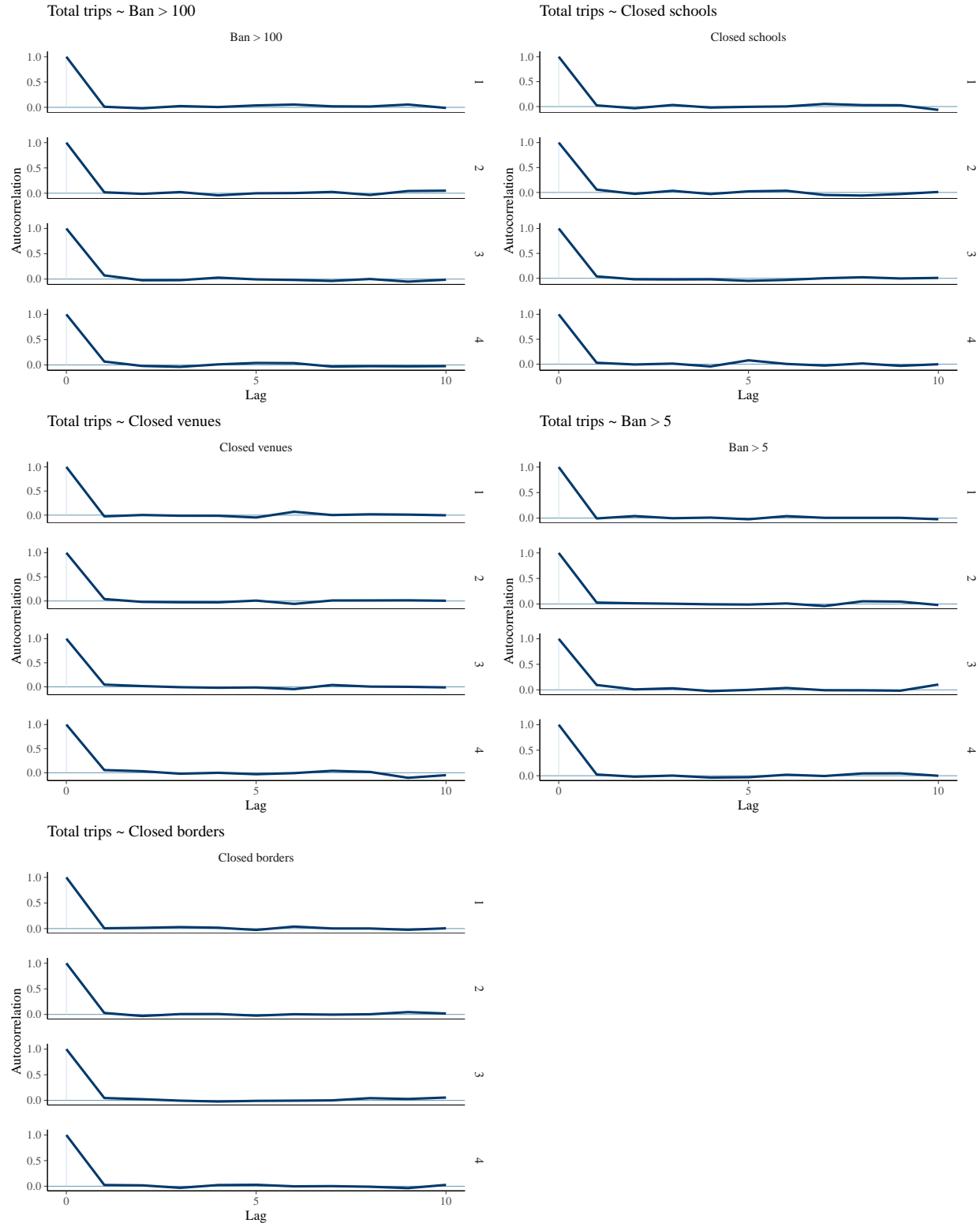


Figure 10: Autocorrelation plots of MCMC samples for each chain of the parameter for the effect of each policy measure on total trips.

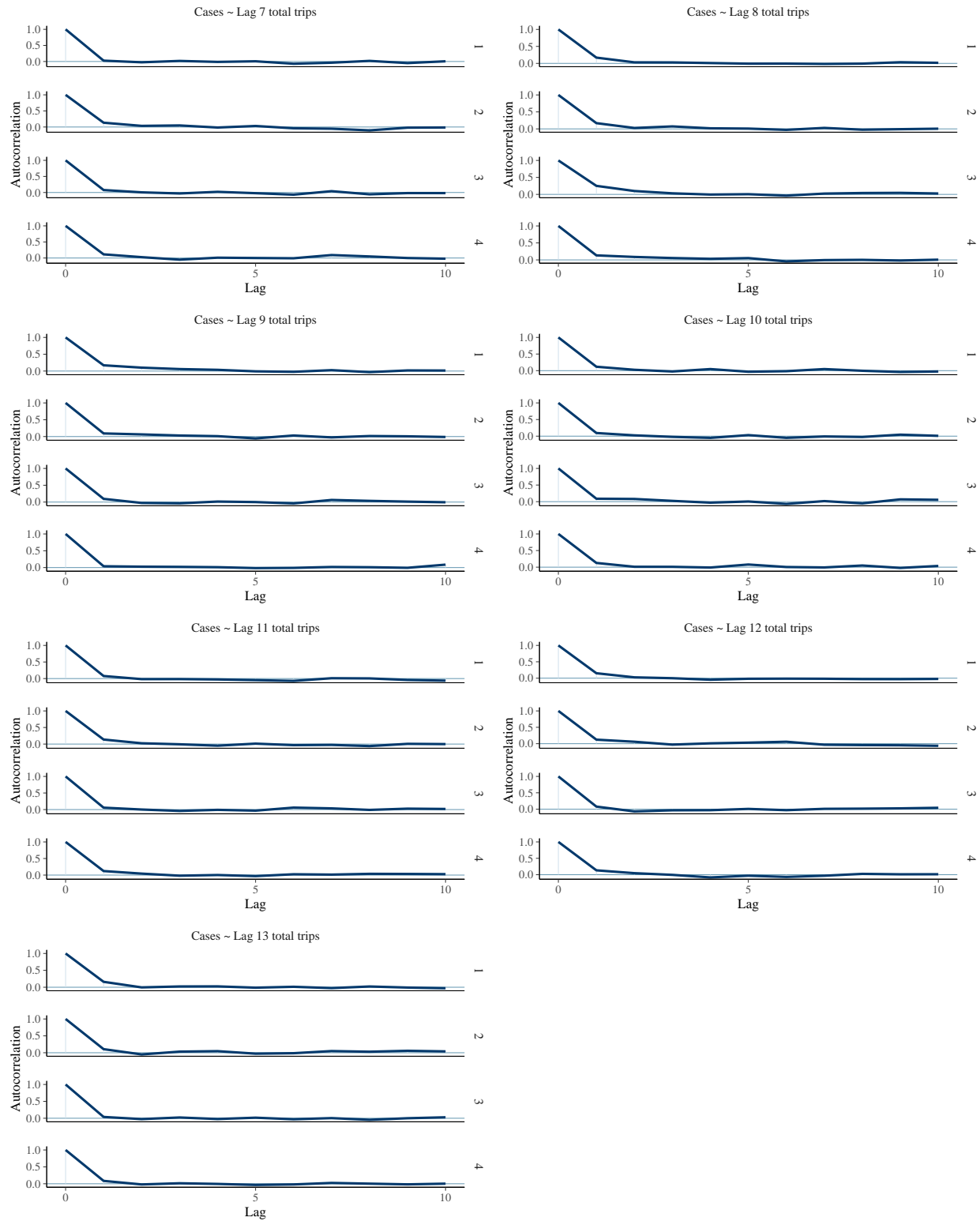


Figure 11: Autocorrelation plots of MCMC samples for each chain of the parameter for the effect of each lag of total trips on the reported number of new cases.

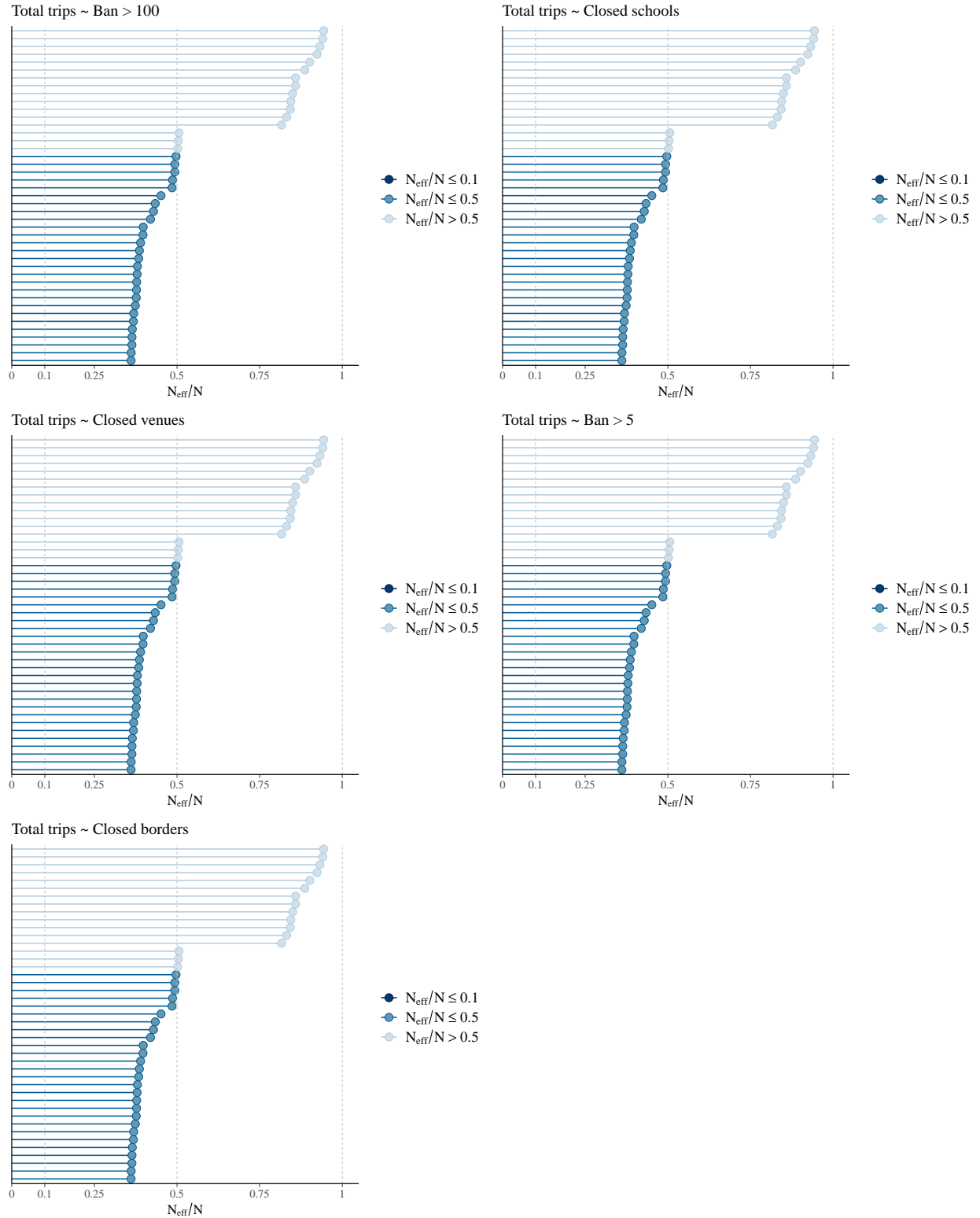


Figure 12: Ratios of effective sample size to total sample size for MCMC samples of the parameter for the effect of each policy measure on total trips.

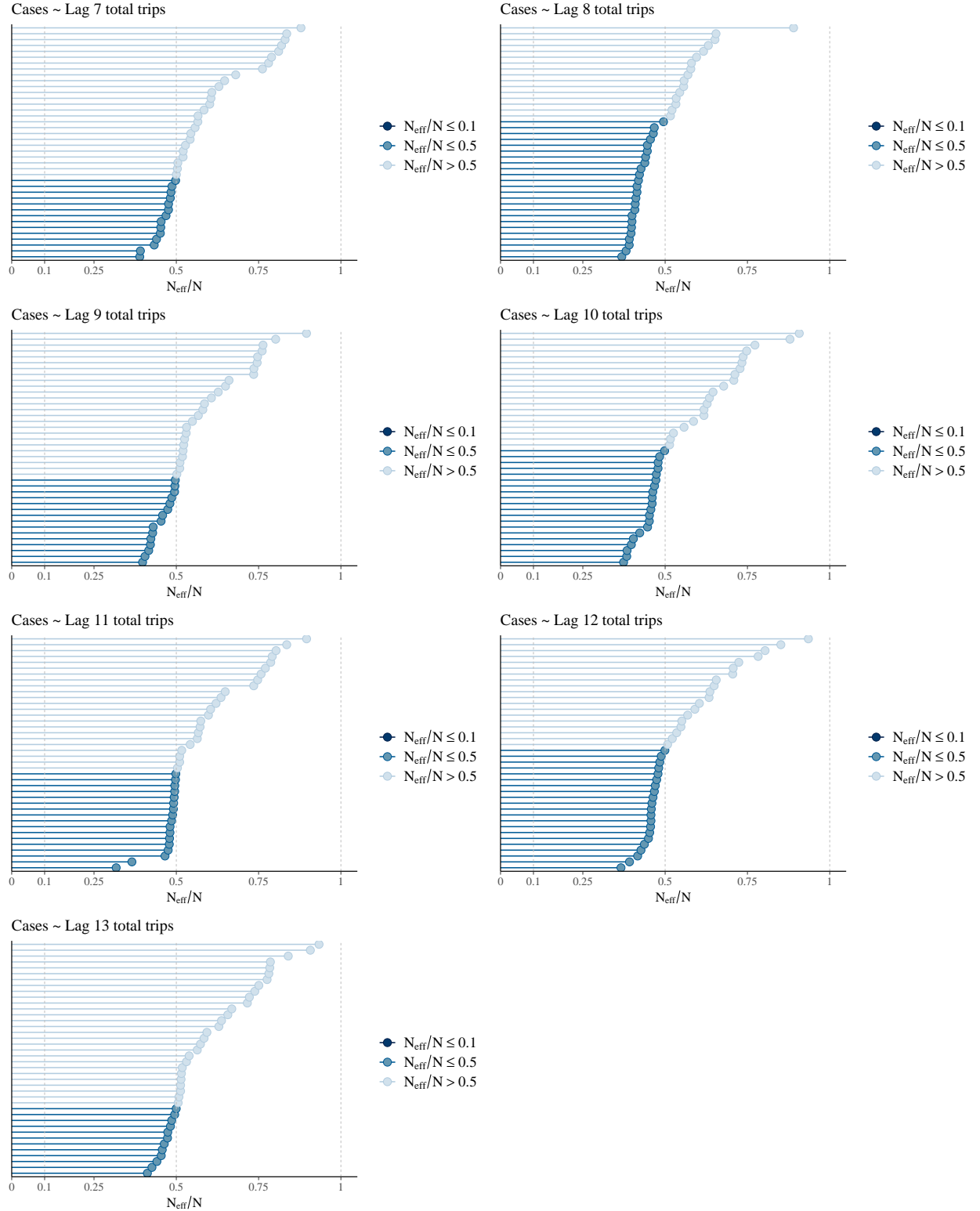


Figure 13: Ratios of effective sample size to total sample size for MCMC samples of the parameter for the effect of each lag of total trips on the reported number of new cases.

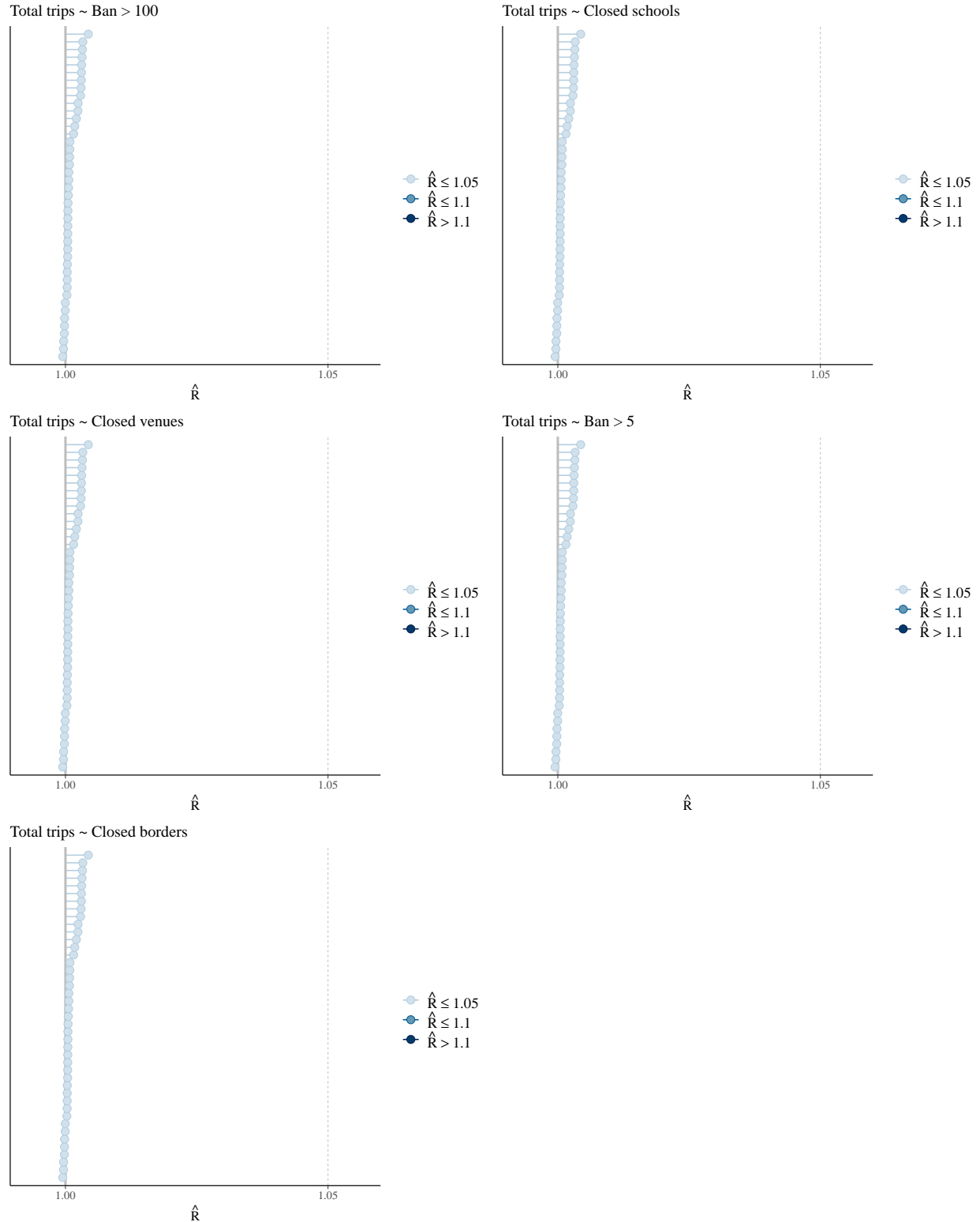


Figure 14:  $\hat{R}$  values for MCMC samples of the parameter for the effect of each policy measure on total trips.

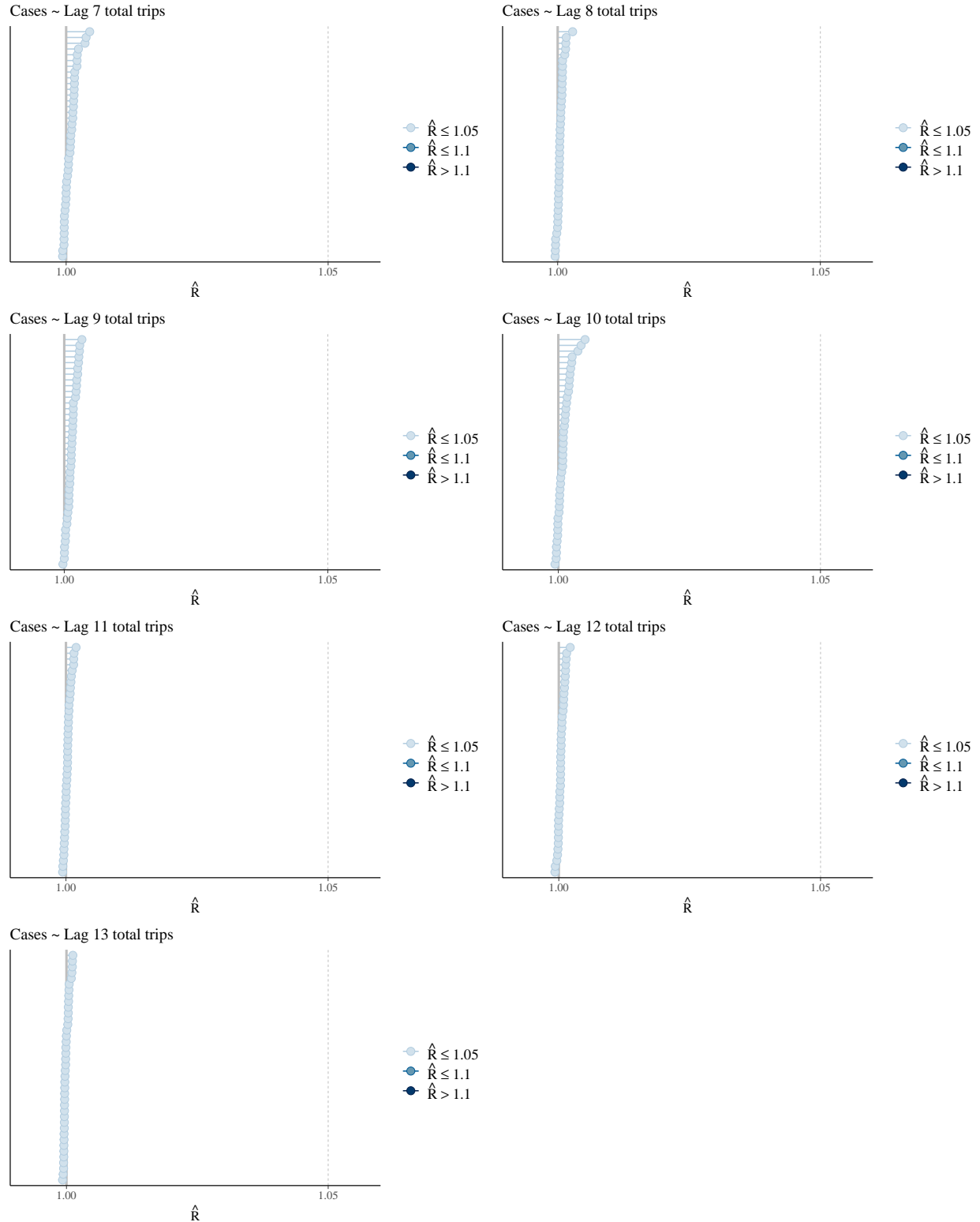


Figure 15:  $\hat{R}$  values for MCMC samples of the parameter for the effect of each lag of total trips on the reported number of new cases.

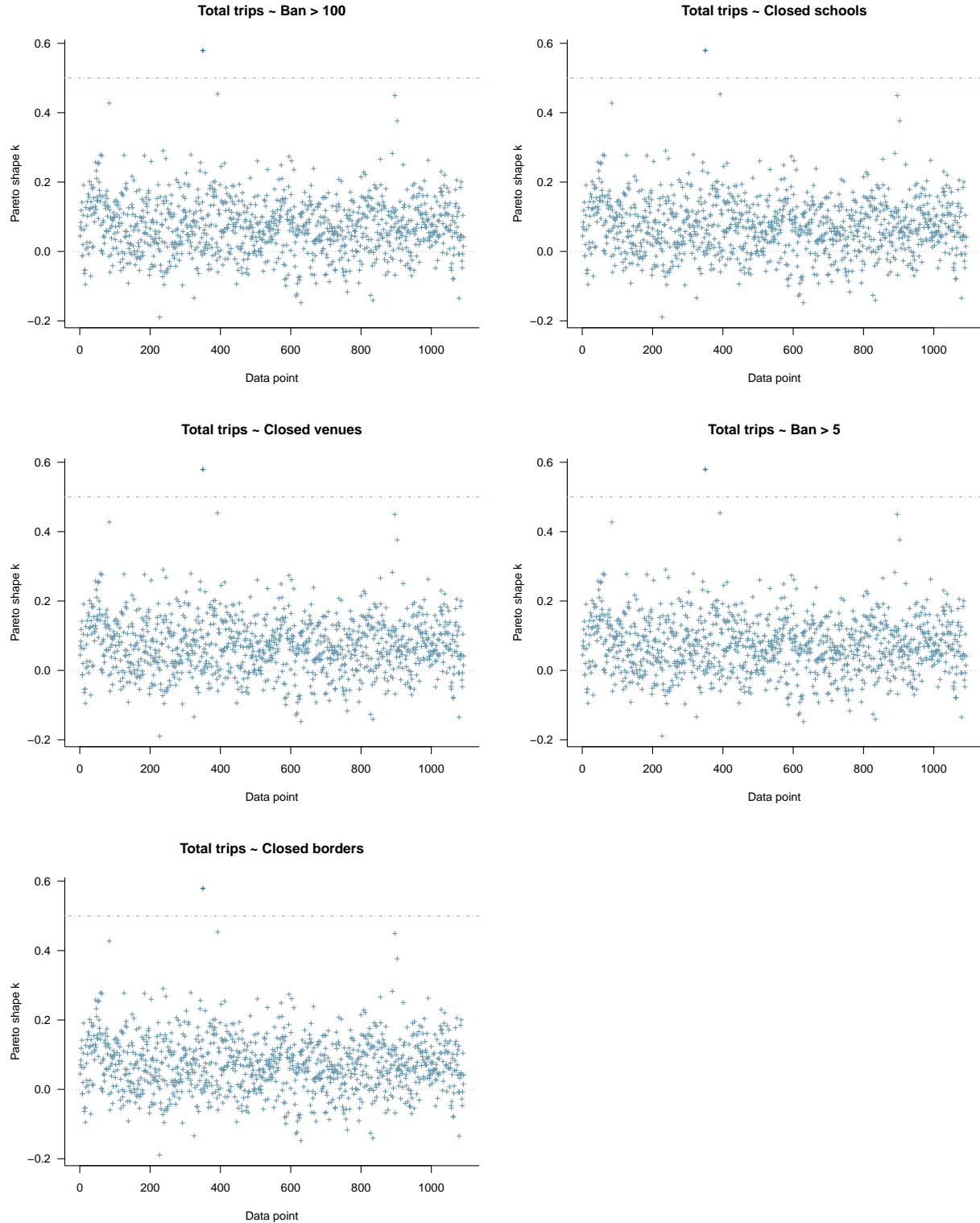


Figure 16: Estimated Pareto tail shape parameter  $k$  against the observation indices for the model of the effect of policy measures on total trips.

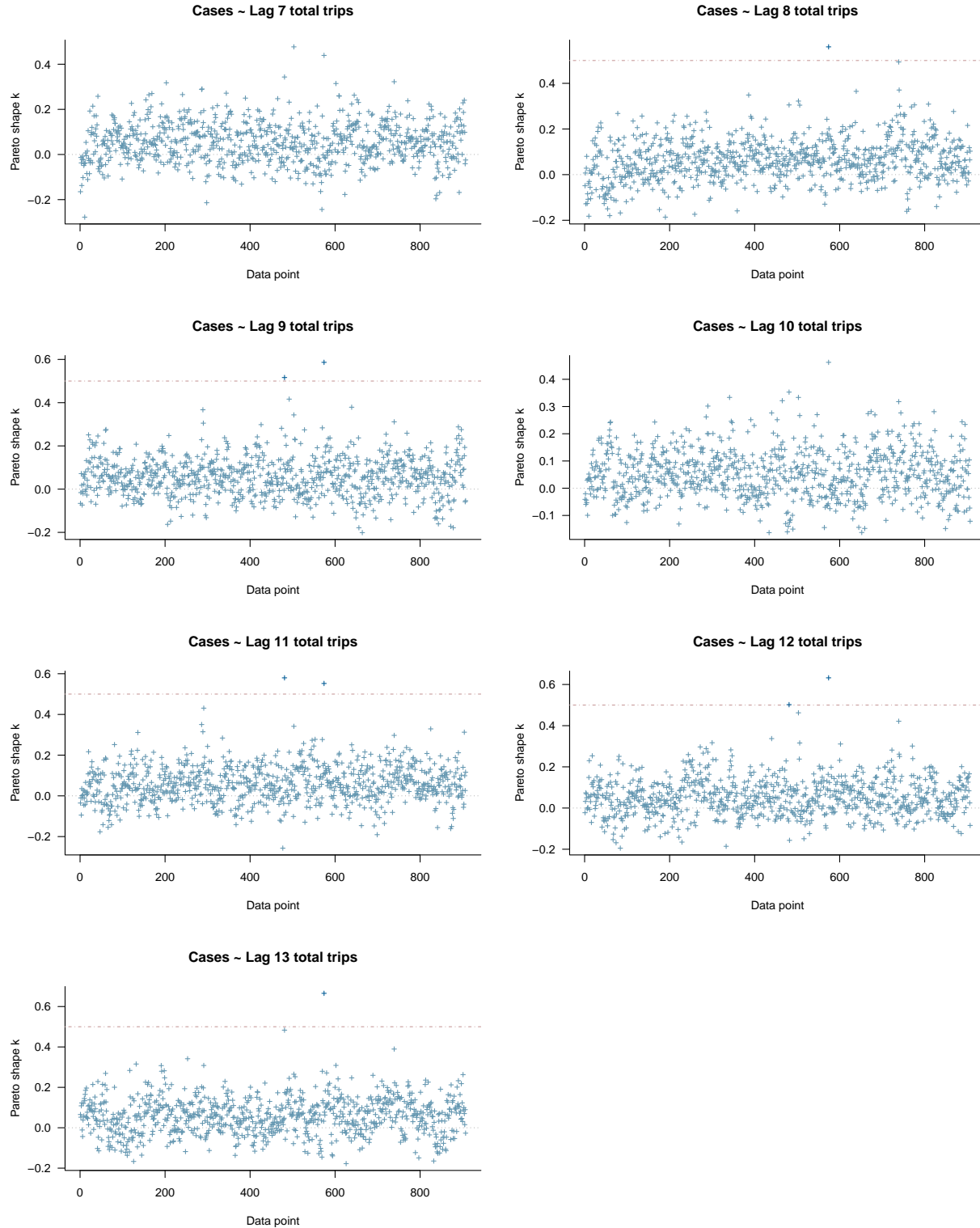


Figure 17: Estimated Pareto tail shape parameter  $k$  against the observation indices for the models of the effect of each lag of total trips on the reported number of new cases.

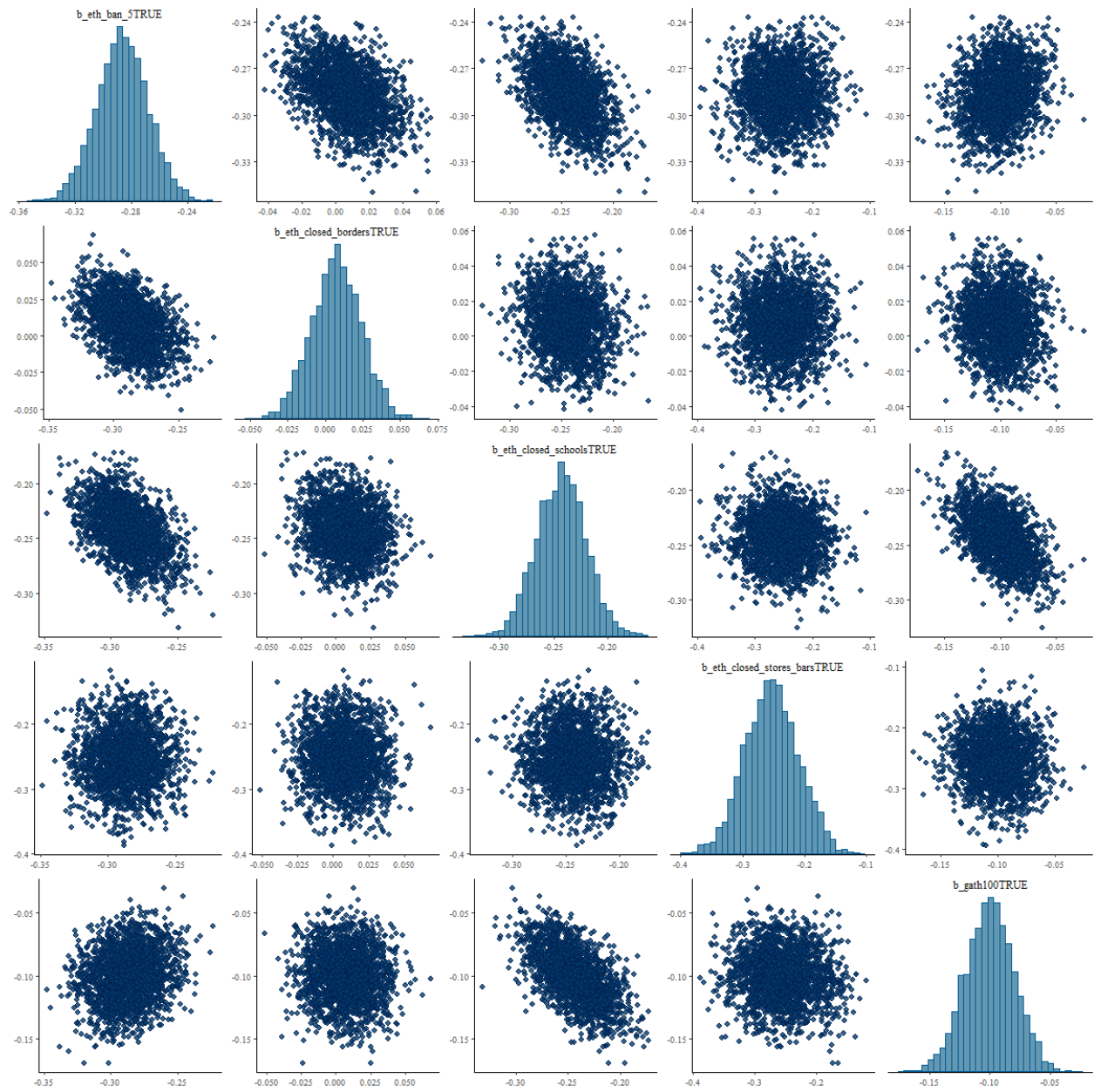


Figure 18: Pairwise bivariate posterior distributions of the policy measure parameters in the model of total trips.

## D Robustness checks

In this section, we test the robustness of our model estimates against alternative specifications.

### D.1 Alternative specifications of time effects

Because the data cover daily observations over a relatively long time period, there are many possible ways of controlling for different time effects. We therefore perform a robustness check of our estimates by re-fitting the models with two alternative specifications of time effects.

Table 4 summarises how the main and alternative model specifications differ. Like the main models, both alternative specifications include weekday fixed effects. The alternative specification (a) uses trend variables of the non-transformed and squared number of days since the first case in each canton was reported (the main specification instead uses the logarithm). Compared to the main specification, it simply postulates a linear and quadratic effect of the number of days since the first case. The alternative specification (b) adds week fixed-effects to the main specification. Thus, it also controls heterogeneity between weeks.

A prior of  $N(0, 1)$  is assigned to the parameters for the linear and quadratic time trends in the second alternative specification. The week fixed-effects in the third alternative specification are assigned a weakly informative prior of  $\text{Half-t}(3, 0, 2.5)$ . All other priors are the same as in the main specification.

The model with the first alternative specification of time effects needed 6000 iterations during MCMC estimation to converge (3000 for samples for warm-up and 3000 samples from its posterior distributions).

Time-effect	Model specification		
	Main	(a)	(b)
Weekday fixed effect	✓	✓	✓
Week fixed-effect			✓
Number of days since 1st reported case		✓	
Squared number of days since 1st reported case		✓	
Log number of days since 1st reported case	✓		✓

Table 4: Specifications of time effects in the models of mobility on policy measures and reported number of new cases on lagged mobility. The symbol "✓" means that a term for the effect is included in the model.

The models of mobility with alternative specifications of time effects give similar estimates as the main specification (Figure 19). Specifically, replacing the logarithmic trend variable with the corresponding linear and squared trends leaves the effects of the policy measures intact (Figure 19a). As expected, adding week fixed effects to the main specification reduces the estimated effects of some policy measures. It also widens the credible intervals for school closures (Figure 19b). Apart from this the estimates are very similar to those of the main model specification. Hence, the estimated policy effects are robust against a range of alternative controls for time effects.

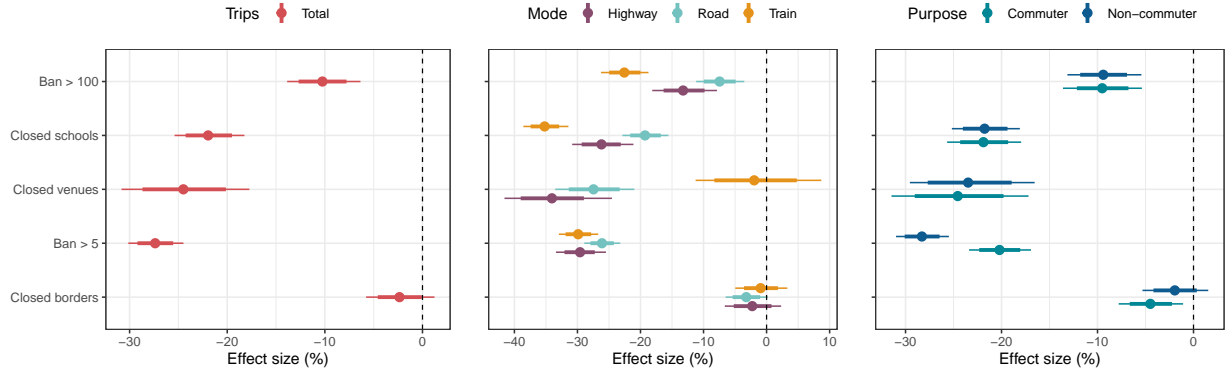
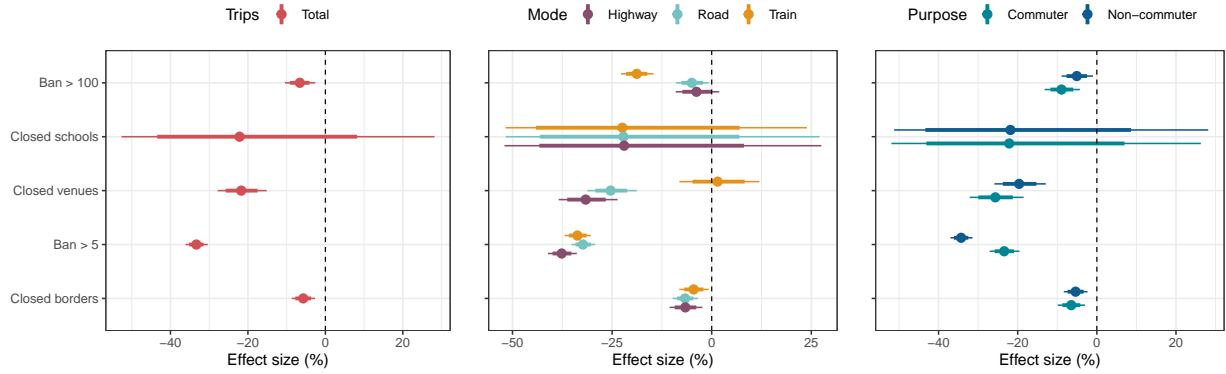
**a****b**

Figure 19: Estimated effect of policy measures on total trips, trips by mode and trip by purpose for three alternative model specifications: **(a)** weekday fixed effects and linear and quadratic trend of the number of days since the first reported case in each canton, and **(b)** weekday fixed effects, week fixed effects, and a trend trend of the log number of days since the first reported case in each canton. Posterior means are shown as dots, while 80 % and 95 % credible intervals are shown as thick and thin bars, respectively. Policy measures are arranged in the order in which they were implemented, shown in Appendix A.

The alternative specifications of time effects are also applied to the model of the reported number of new cases on lagged mobility. Figure 20 shows their predictions of the percentage change in the reported number of new cases given a 1 % decrease in mobility lagged by 7–13 days. Replacing the logarithmic trend variable with linear and quadratic trends does not alter the estimated relationship between the mobility variables and reported case growth substantially (Figure 20a). The predicted reduction in case growth given decrease in total trips is stronger than

in the main specification whereas the predicted reduction given decreases in commuter trips is slightly weaker. Adding week fixed-effects to the main specification leads to a smaller predicted change in reported case growth given reductions in mobility (Figure 20b). For some lags of the mobility variables is the predicted reduction not statistically distinguishable from zero. However, decreases in mobility still predicts reductions in reported case growth for the larger lags.

Altogether, the robustness checks show that the predicted reductions in reported cases given decreases in mobility are robust to alternative specifications of time effects.

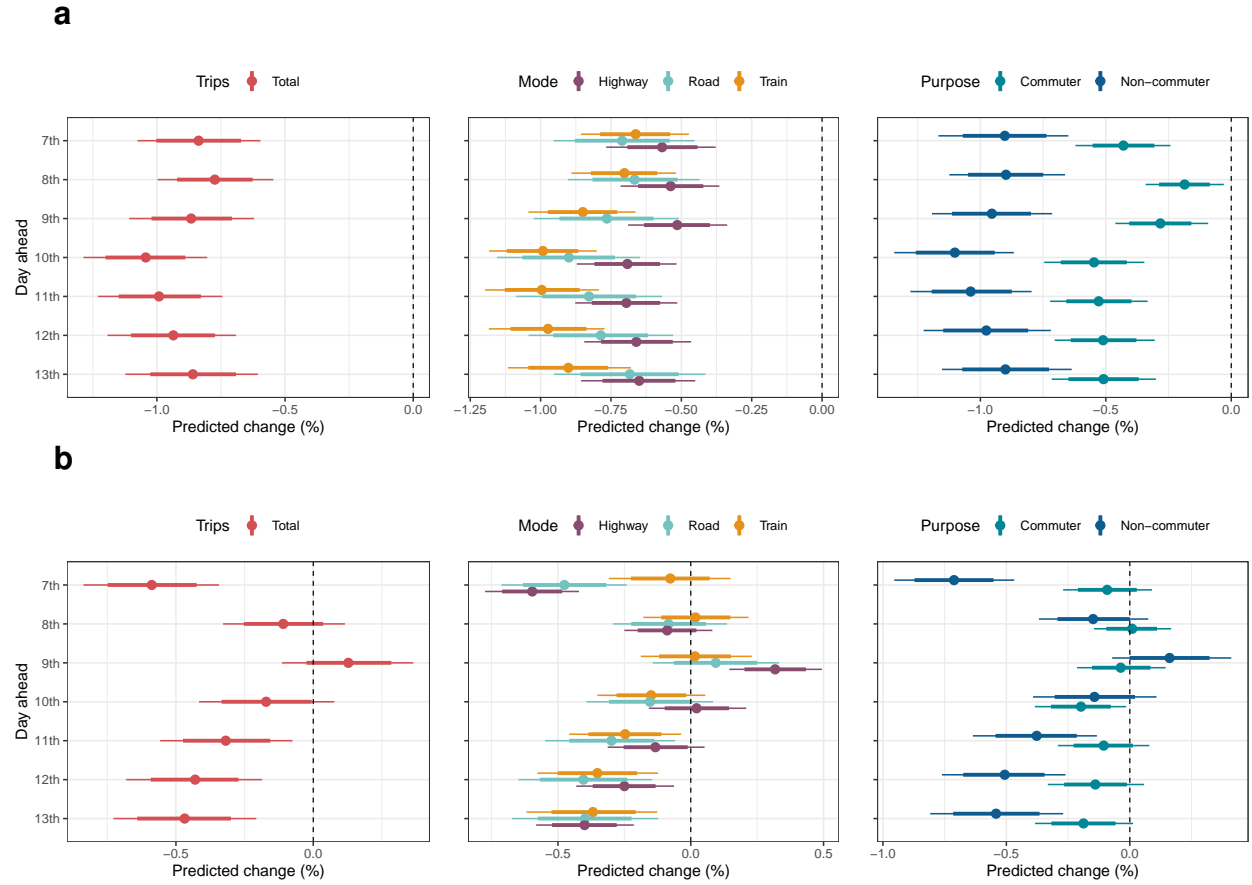


Figure 20: Predicted change in reported COVID-19 cases given a 1 % reduction of lagged total trips, trips by mode, and trips by purpose for alternative specifications of time effects: (a) weekday fixed effects and linear and quadratic trend of the number of days since the first reported case in each canton, and (b) weekday fixed effects, week fixed effects, and a trend trend of the log number of days since the first reported case in each canton. Posterior means are shown as dots, while 80 % and 95 % credible intervals are shown as thick and thin bars, respectively. Policy measures are arranged in the order in which they were implemented, shown in Appendix A.

## D.2 Controlling for the number of tests

The number of positive reported cases depends on the number of tests performed, which can vary over the course of the pandemic. We therefore re-estimate our models of the reported number of new cases on lagged mobility while controlling for the number of tests performed every day. This is based on the assumption that cantons might not conduct equally many tests each day. Instead, the number of tests that each cantons carry out might be determined by their population size and other relevant risk factors in their population. Since test availability determines the number of positive tests that can be detected, we extend the model of the relation between mobility and the reported case growth with the number of daily tests per canton.

To the best of our knowledge, there exists no data on the number of tests conducted per day in each canton of Switzerland but only in the country as a whole. We therefore estimate the number of daily tests conducted per canton with the the number of daily tests in the whole of Switzerland standardized to the canton population shares. That is, we divide the number of daily tests in Switzerland as a whole with each cantons population share.

Formally, let  $u_{it}$  be the true unknown number of tests reported in canton  $i$  in day  $t$  and let  $u_t = \sum_{i=1}^N u_{it}$  be the total and observed number of reported tests in the country in day  $t$ . We estimate the number of tests in canton  $i$  in day  $t$  with

$$\hat{u}_{it} = u_t \times \frac{E_i}{\sum_{i=1}^N E_i}, \quad (12)$$

where  $E_i$  is the population in canton  $i$ , and  $\sum_{i=1}^N E_i$  is the population in the country. The estimate  $\hat{u}_{it}$  thereby approximates the number of COVID-19 tests conducted in each canton and day under the assumption that the number of daily tests per canton is proportionate to the share of the population that lives in each canton. We include the logarithm of  $\hat{u}_{it}$  in the model so that it estimates the percentage change in the reported number of new cases when the estimated number of daily tests increases by 1 %. We assign the log-transformed variable a prior of  $N(1, 1)$ , meaning that we

expect the effect size to be 1 % on average, but likely not negative or larger than 2 %.

After controlling for the number of daily tests per canton, decreases in mobility lagged by 10–13 days still predict reductions in the reported number of new cases. Our findings are therefore qualitatively the same for the majority of lags. However, the above analysis should be interpreted with caution as it may be subject to post-treatment bias. The reason is as follows. Given an increase in mobility, hospitals may in anticipation of a growth in cases in the near future start to carry out more tests. Then, for a given day, the number of tests is (partially) an outcome of previous levels of mobility. As a consequence, variation in the reported number of new cases that should be attributed to changes in mobility gets incorrectly attributed to changes in the number of tests. As a consequence, the parameter estimate for lagged mobility is biased. Such post-treatment bias might explain the near-zero and positive estimates observed for some lags of mobility after controlling for the number of tests.

## E Modeling extensions

This section includes extensions of the models featured in the paper. Estimation details are in Appendix G.

### E.1 Accounting for the spatial dependence in mobility among neighboring cantons

Our main models treat mobility as being independent across cantons. Modeling cross-sectional units as independent is a conventional approach in panel and longitudinal data analysis. However, one would reasonably expect that the level of mobility is similar for neighboring cantons but not so similar for geographically distant cantons. If a dependence in mobility between cantons is not modeled, it will enter the error term, violating the assumption that error terms are independent across cantons. For this purpose, we extend the mobility model with a spatial random effect that captures the similarity in mobility among neighboring cantons prior to any policy measure.

Let  $\phi_i^{(k)}$  be a spatial random effect for canton  $i$  that has an additive effect on mobility variable  $k$  on the log scale. The model for the effect of the policy measure on mobility variable  $k$  is then given by

$$\log \mathbb{E}[M_{itk} | \eta_{it}^{(k)}, E_i] = \log E_i + \alpha^{(k)} + \theta_i^{(k)} + \phi_i^{(k)} + \delta_{w(t)}^{(k)} + \gamma^{(k)} \log z_{it} + \gamma_B^{(k)} \log \bar{z}_i + \sum_{l=1}^L \beta_l^{(k)} d_{itl}. \quad (13)$$

The spatially-extended model may be viewed as a longitudinal version of the Besag-York-Mollié (BYM) model<sup>65</sup> commonly used for disease mapping applications in epidemiology. The term “disease mapping” refers to statistical methods that estimates the spatial correlation between observations and where interest lies in the distribution of a disease over geographical units. The BYM model, in turn, is a Bayesian hierarchical Poisson regression model with two types of random ef-

fects: (1) random effects that capture spatial correlation between units, and (2) random effects that captures unobserved heterogeneity between units<sup>66</sup>. Our spatially extended model adapts the original BYM model with the use of a negative binomial distribution to account for the overdispersion in the trip counts. It also adapts the original BYM model by treating the random effects for unobserved heterogeneity as Mundlak-style correlated random effects. This enables us to get correct inference even if the date that each cantons first case is reported depends on unobserved canton-specific factors.

As the original BYM model, we use an intrinsic conditional auto-regressive (ICAR) model as a prior on the spatial random effect  $\phi_i$ . The ICAR model of the conditional distribution of each  $\phi_i$  is

$$\phi_i \mid \{\phi_j : j \in \mathcal{N}_i\} \sim \mathcal{N} \left( \frac{1}{|\mathcal{N}_i|} \sum_{j \in \mathcal{N}_i} \phi_j, \frac{1}{\tau |\mathcal{N}_i|} \right), \quad (14)$$

where  $\mathcal{N}_i$  is the set of neighbors of canton  $i$ , meaning the cantons that share a border with the canton, and  $|\mathcal{N}_i|$  denotes the cardinality of  $\mathcal{N}_i$ , that is, its number of neighbours. For practical implementation, the sets of neighbors can be constructed by defining a symmetric  $N \times N$  adjacency matrix whose element in row  $i$  and column  $j$  equals 1 if cantons  $i$  and  $j$  share a common border, and 0 otherwise.

The ICAR model states that each  $\phi_i$  is conditionally Gaussian with mean equal to the average of its neighbors spatial random effects and a variance that decreases with more neighbors. The term  $\tau$  is a hyperparameter for the variance of the composite random effect  $v_i = \theta_i + \phi_i$ , where  $\theta_i$  is the random effect for unobserved heterogeneity. Based on derivations in<sup>77</sup>, the joint distribution of  $\phi = (\phi_1, \dots, \phi_N)$  is proportional to a particular pairwise difference form:

$$p(\phi \mid \tau) \propto \exp \left( -\frac{\tau}{2} \sum_{i,j:j \in \mathcal{N}_i} (\phi_i - \phi_j)^2 \right) = \exp \left( -\frac{\tau}{2} \phi^\top \mathbf{Q} \phi \right). \quad (15)$$

Here,  $\mathbf{Q}$  is the precision matrix, e. g., the inverse spatial covariance matrix, that has entries

$$Q_{i,j} = \begin{cases} |\mathcal{N}_i|, & \text{if } i = j, \\ -1, & \text{if } j \in \mathcal{N}_i, \\ 0, & \text{else.} \end{cases}$$

The pairwise difference form (15) shows that the ICAR model penalises large differences in the values of neighboring cantons spatial random effects. Hence, finding the values of  $\{\phi_i\}_{i=1}^N$  that minimize these differences leads to local spatial smoothing<sup>78</sup>. However, the distributions in (14) and (15) are improper priors since they define the value of each cantons spatial effect relative to its neighbors. As a consequence, the priors do not identify the overall mean among  $\{\phi_i\}_{i=1}^N$ . To solve this, the soft constraint  $N^{-1} \sum_{i=1}^N \phi_i \sim \mathcal{N}(0, 0.001)$  is used.

Another problem is that the random effects  $\phi_i$  and  $\theta_i$  cannot be separately identified. Thus, heterogeneity across cantons that should be attributed to  $\theta$  will be modeled as spatial correlation by  $\phi$  even when no spatial dependence is present. To solve this issue, we use the reformulated BYM2 model<sup>56</sup>. It involves a scaling<sup>79</sup> and reparameterization<sup>80</sup> of  $\mathbf{v} = \theta + \phi$ , explained next.

Let  $\phi_i^* := \phi_i / \sqrt{\kappa}$  be the spatial random effect for canton  $i$  after scaling. The scaling factor  $\kappa$  is calculated from the neighborhood structure over all cantons and ensures that  $\mathbb{V}[\phi_i^*] \approx \mathbb{V}[\theta_i] \approx 1$  for each canton  $i$ . The scaled reparameterization of  $v_i = \theta_i + \phi_i$  is

$$\frac{1}{\sqrt{\tau}} \left( (\sqrt{1 - \varphi}) \theta_i + \sqrt{\varphi} \phi_i^* \right). \quad (16)$$

The corresponding covariance matrix of  $\mathbf{v} = (v_1, \dots, v_N)$  is

$$\mathbb{V}[\mathbf{v} | \tau, \varphi] = \frac{1}{\tau} \left( (1 - \varphi) \mathbf{I} + \varphi \mathbf{Q}_*^- \right). \quad (17)$$

Here,  $\mathbf{Q}_*^-$  is the generalized inverse of the scaled precision matrix  $\mathbf{Q}_*$ ,  $\varphi \in [0, 1]$  is a mixing pa-

rameter, and  $1/\tau$  is the marginal variance of log relative mobility that is explained by the combined random effect  $\boldsymbol{v}$ . The fraction of this variance explained by the canton random effect  $\boldsymbol{\theta}$  and the scaled spatial random effect  $\boldsymbol{\phi}^*$  are  $(1 - \varphi)$  and  $\varphi$ , respectively<sup>79</sup>.

Summarizing, the random effect  $\boldsymbol{\theta}$  for between-canton heterogeneity has prior distribution  $\text{MVN}(\mathbf{0}, \mathbf{I})$  and the spatial random effects  $\boldsymbol{\phi}$  has prior marginal distribution  $\text{MVN}(\mathbf{0}, \mathbf{Q}_*^-)$  and prior conditional distribution given by (14) for each  $\phi_i$ . See Riebler et al.<sup>56</sup> for details. Replacing  $v_i = \theta_i + \phi_i$  in (13) with (16) gives the explicit equation for the model of mobility variable  $k$  with the BYM2 spatial random effect.

Accounting for potential spatial dependence in mobility among neighboring cantons does not alter the estimates of the policies (Figure 21). In other words, the spatial dependence in baseline mobility is low. We therefore do not include the BYM2 spatial random effect in our main models.

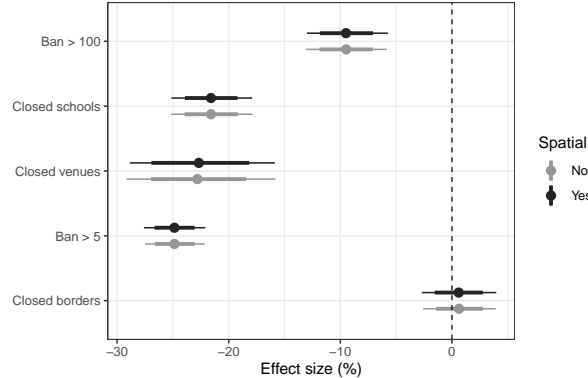


Figure 21: Estimated effect of policy measures on total trips with and without a BYM2 ICAR random effect for spatial dependence between neighboring cantons. Posterior means are shown as dots, while 80 % and 95 % credible intervals are shown as thick and thin bars, respectively. Policy measures are arranged in the order in which they were implemented, shown in Appendix A.

## E.2 Accounting for the dependence between the mobility variables

The variables for trips by mode or reason are different subsets of the total trips. As a result, the trip variables are dependent on each other. One way in which this dependence could arise is through the variation in baseline trip counts across cantons prior to any reported COVID-19

case and policy measure. As an example, we would expect the cross-canton variation in baseline commuting trips to be correlated with the cross-canton variation in baseline non-commuting trips. Since each regression equation's canton random effect  $\boldsymbol{\theta}^{(k)} = (\theta_1^{(k)}, \theta_2^{(k)}, \dots, \theta_N^{(k)})$  gives the cross-canton variation in mobility variable  $k$  at baseline, we can estimate the dependence between the mobility variables at baseline with the correlation coefficient between the canton random effects. To do so, we model  $\boldsymbol{\theta}^{(1)}, \boldsymbol{\theta}^{(2)}, \dots, \boldsymbol{\theta}^{(K)}$  as jointly multivariate Gaussian distributed:

$$\begin{bmatrix} \boldsymbol{\theta}^{(1)} \\ \boldsymbol{\theta}^{(2)} \\ \vdots \\ \boldsymbol{\theta}^{(K)} \end{bmatrix} \sim \text{MVN}(\mathbf{0}, \boldsymbol{\Omega}_M), \quad \boldsymbol{\Omega}_M = \begin{bmatrix} \sigma_{\boldsymbol{\theta}^{(1)}}^2 \mathbf{I} & \sigma_{\boldsymbol{\theta}^{(2)} \boldsymbol{\theta}^{(1)}} \mathbf{I} & \dots & \sigma_{\boldsymbol{\theta}^{(K)} \boldsymbol{\theta}^{(1)}} \mathbf{I} \\ \sigma_{\boldsymbol{\theta}^{(1)} \boldsymbol{\theta}^{(2)}} \mathbf{I} & \sigma_{\boldsymbol{\theta}^{(2)}}^2 \mathbf{I} & \dots & \sigma_{\boldsymbol{\theta}^{(K)} \boldsymbol{\theta}^{(2)}} \mathbf{I} \\ \vdots & \vdots & \ddots & \vdots \\ \sigma_{\boldsymbol{\theta}^{(1)} \boldsymbol{\theta}^{(K)}} \mathbf{I} & \sigma_{\boldsymbol{\theta}^{(2)} \boldsymbol{\theta}^{(K)}} \mathbf{I} & \dots & \sigma_{\boldsymbol{\theta}^{(K)}}^2 \mathbf{I} \end{bmatrix} = \boldsymbol{\Sigma}_M \otimes \mathbf{I}, \quad (18)$$

where  $\sigma_{\boldsymbol{\theta}^{(k)}}^2$  is the variance of  $\boldsymbol{\theta}^{(k)} = (\theta_1^{(k)}, \theta_2^{(k)}, \dots, \theta_N^{(k)})$  of regression equation  $k = 1, 2, \dots, K$ , the term  $\sigma_{\boldsymbol{\theta}^{(k)} \boldsymbol{\theta}^{(p)}}$  is the corresponding covariance between  $\boldsymbol{\theta}^{(k)}$  and  $\boldsymbol{\theta}^{(p)}$  from regressions equations  $k$  and  $p$ , respectively, and the  $K \times K$  covariance matrix  $\boldsymbol{\Sigma}_M$  contains these variance and covariance terms. Moreover,  $\mathbf{I}$  is an  $N \times N$  identity matrix and the symbol  $\otimes$  denotes the Kronecker product.

We then obtain the correlations between all pairs of canton random effects for each pair of  $k, p = 1, 2, \dots, K, k \neq p$ , by computing the Pearson coefficient

$$\rho_{\boldsymbol{\theta}^{(k)} \boldsymbol{\theta}^{(p)}} = \frac{\sigma_{\boldsymbol{\theta}^{(k)} \boldsymbol{\theta}^{(p)}}}{\sqrt{\sigma_{\boldsymbol{\theta}^{(k)}}^2 \sigma_{\boldsymbol{\theta}^{(p)}}^2}}. \quad (19)$$

The correlation coefficients are collected as off-diagonal elements in the  $K \times K$  correlation matrix  $\mathbf{R}_M$  corresponding to  $\boldsymbol{\Sigma}_M$  and can be interpreted as summaries of the dependence between the mobility variables' baseline relative trip counts across cantons in the absence of any policy measure and reported COVID-19 case. By modeling this dependence, we obtain more precise estimates of uncertainty in parameter values than estimating each mobility variable's regression equation separately. The approach is analogous to that of seemingly unrelated regressions<sup>81</sup>, except that

each regression model is a negative binomial generalized mixed model with a log-link.

Figure 22 shows estimates of the effect of the policy measures on mobility from the multivariate model (Figure 22a) against the estimates from the separate regressions per mobility variables for which the correlation between their canton random effects is not modeled (Figure 22b). Comparing the multivariate and separate regressions, we find that the point estimates given by the posterior means are practically identical. There is a small tendency of the credible intervals in the multivariate model to be tighter. Note that estimating the multivariate model requires considerably more computational runtime.

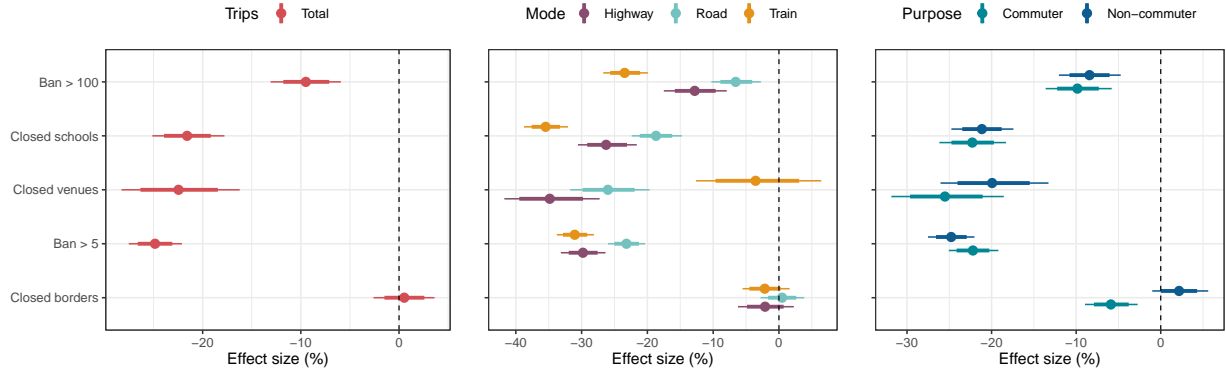
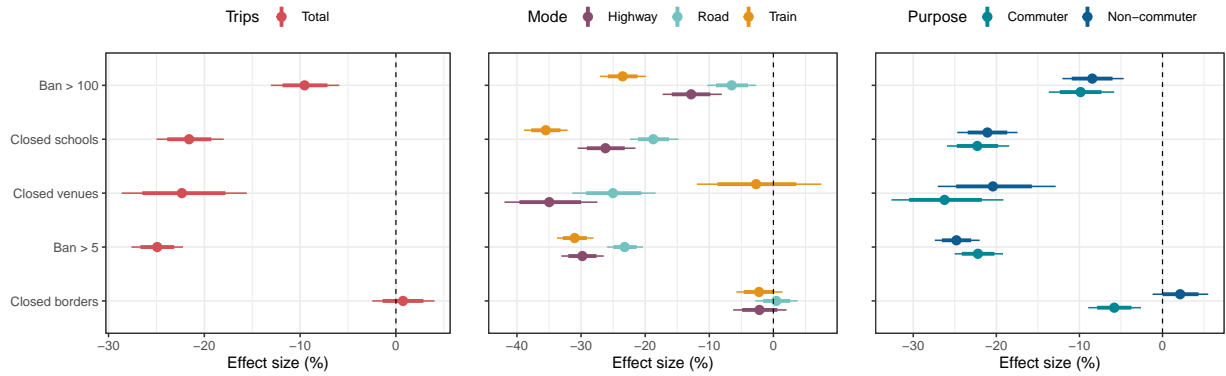
**a****b**

Figure 22: Estimated effects of policy measures on total trips, trips by mode, trips by purpose from (a) the joint multivariate model over all mobility variables, and (b) the separate regressions per mobility variable. The joint multivariate model estimates the correlation between the baseline levels of the mobility variables across cantons by modeling the canton random effects as drawn from a multivariate Gaussian distribution. Posterior means are shown as dots, while 80 % and 95 % credible intervals are shown as thick and thin bars, respectively. Policy measures are arranged in the order in which they were implemented, shown in Appendix A.

## F Mediation analysis of the role of mobility in the effect of policy measures on reported cases

We perform a mediation analysis to decompose the effects of policy measures on reported COVID-19 cases into (1) their direct effects, meaning the part of their effects that is due to behavioral adaptions not related to mobility, and (2) their indirect effects, meaning the part of their effects that is explained by changes in mobility. The mediation analysis is performed by combining our two regression models into a structural equation model. Estimation details are provided in Appendix G.

### F.1 Mediation model

The structural equation model consists of the mediation model

$$\begin{aligned}
 \log \mathbb{E}[M_{i,t-s,k} \mid \eta_{i,t-s}^{(k,s,M)}, E_i] &= \mu(M_{i,t-s,k}) \\
 &= \log E_i + \alpha_i^{(k,s,M)} + \delta_{w(t-s)}^{(k,s,M)} + \gamma^{(k,s,M)} \log z_{i,t-s} + \sum_{l=1}^L \beta_l^{(k,s)} d_{i,t-s,l} \\
 \alpha_i^{(k,s,M)} &= \alpha^{(k,s,M)} + \theta_i^{(k,s,M)} + \gamma_B^{(k,s,M)} \overline{\log z_i}
 \end{aligned} \tag{20}$$

and the outcome model

$$\begin{aligned}
 \log \mathbb{E}[Y_{it} \mid \eta_{it}^{(k,s,Y)}, E_i] &= \mu^{(k,s)}(Y_{it}) \\
 &= \log E_i + \alpha_i^{(k,s,Y)} + \delta_{w(t)}^{(k,s,Y)} + \gamma^{(k,s,Y)} \log z_{it} + \psi_{ks} \log m_{i,t-s,k} + \sum_{l=1}^L \lambda_l^{(k,s)} d_{i,t-s,l} \\
 \alpha_i^{(k,s,Y)} &= \alpha^{(k,s,Y)} + \theta_i^{(k,s,Y)} + \gamma_B^{(k,s,Y)} \overline{\log z_i} + \psi_{ks,B} \overline{\log m_{ik}}
 \end{aligned} \tag{21}$$

For notation, the bar again denotes the average value of an expression. The superscripts  $M$  and  $Y$  are added to indicate that the parameter values are generally different for the mediation model and outcome model with the same mobility variable  $k$  lagged by  $s$  days. The conditional variance of  $M_{i,t-s,k}$  and  $Y_{it}$  is given by

$$\mathbb{V}[M_{i,t-s,k} | \eta_{i,t-s}^{(k,s,M)}, E_i, \zeta^{(k,s,M)}] = \mu(M_{i,t-s,k}) \left( 1 + \frac{\mu(M_{i,t-s,k})}{\zeta^{(k,s,M)}} \right) \quad (22)$$

and

$$\mathbb{V}[M_{i,t-s,k} | \eta_{it}^{(k,s,Y)}, E_i, \zeta^{(k,s,Y)}] = \mu^{(k,s)}(Y_{it}) \left( 1 + \frac{\mu^{(k,s)}(Y_{it})}{\zeta^{(k,s,Y)}} \right). \quad (23)$$

Here,  $\zeta^{(k,s,M)}$  and  $\zeta^{(k,s,Y)}$  is the overdispersion parameter from the mediation model and outcome model, respectively, in which mobility variable  $k$  is lagged by  $s$  days.

The mediation model is identical to the model that links policy measures to mobility, but has lagged values of all time-varying variables since their effects on the reported number of new cases are delayed. The outcome model is the same as the model that links mobility to reported cases, but now also includes the policy measures. The reason for this is that the structural equation model shall estimate (1) the effects of mobility conditional on the policy measures, and (2) the effects of the policy measures conditional on mobility. Here, (1) gives the mediation effect of mobility that enables us to estimate the indirect effect of policy measures via mobility, and (2) gives the direct effect of policy measures that explained by other behavioral adaptions. The added superscripts  $m$  and  $y$  signifies that the parameters generally take different values in the mediation model and outcome model.

To facilitate the interpretation of our results, we state how the parameters of interest shall be interpreted in the mediation analysis:

- $\beta_l^{(k,s)}$  is the effect of policy measure  $l$  on the log expected number of trips on mobility

variable  $k$ .

- $\lambda_l^{(k,s)}$  is the direct effect of policy measure  $l$  lagged by  $s$  days on the log expected number of reported cases, conditional on mobility variable  $k$  lagged by  $s$  days and the other policy measures lagged by  $s$  days. Formally, this is the change that would occur in the reported number of new cases if (lagged) policy measure  $l$  would have been implemented but mobility would not have changed as a consequence of policy measure  $l$ .
- $\psi_{ks}$  is the expected percentage change in the reported number of new cases as the number of trips on mobility variable  $k$  lagged by  $s$  days increases by 1 %, conditional on all policy measures lagged by  $s$  days being held fixed.
- $\beta_l^{(k,s)} \times \psi_{ks}$  is the indirect effect of policy measure  $l$  via mobility variable  $k$ , both lagged by  $s$  days, on the log expected reported number of new cases. The indirect effect gives the expected change that would occur in the reported number of new cases if policy measure  $l$  lagged by  $s$  days would always have been implemented but mobility variable  $k$  lagged by  $s$  days would have changed as if the policy measure would vary as in the data.
- $\lambda_l^{(k,s)} + \beta_l^{(k,s)} \times \psi_{ks}$  is the total effect of policy measure  $l$  lagged by  $s$  days on the log expected number of reported cases. It is the effect of policy measure  $l$  with the mobility variable  $k$  changing as a consequence of implementing the policy measure. Hence, the total effect gives the change in the reported number of new cases due to any behavioral adaption.

As shown in the above, we compute the indirect effect using the product method<sup>82</sup> and sum the direct and indirect effect to obtain the total effect. This is applicable to linear Bayesian multilevel models with random intercepts and no mediator-treatment interaction<sup>83</sup> (i.e., no treatment-moderated mediation), as the models of this study.

We check the assumption of no treatment-mediator interaction by, for every lag of 7–13 days, re-estimating the outcome model (21) with an interaction term between each policy measure and

the mobility variable. We find that the parameters of the interaction terms have point estimates close to zero with some of the credible intervals covering zero. We take this as sufficient evidence of no treatment-mediator interaction and, therefore, proceed with the outcome model without such terms.

The directed acyclic graph in Figure 23 visualises the relationships between the variables in the structural equation model at a given day. For simplicity, we denote weekday, time and unobserved canton factors lagged by  $s$  days with the vector  $\mathbf{X}_{i,t-s}$ . The structural relationships among the variables are as follows: At day  $t$ , the weekday, the number of days that has passed since the first case was reported in the canton, and unobserved canton-specific factors jointly determine the number of trips in the canton on each mobility variable and whether each policy measure is implemented in the canton that day. The weekday, number of days that has passed since the first reported case, and unobserved canton-specific factors also determine the reported number of new cases, but with a lag of  $s$  days due to incubation periods and reporting delay. Whether a policy measure is implemented in a canton at day  $t$  affects the trip count on each mobility variable in same the canton that day (path  $\beta_l^{(k,s)}$ ). Given the implementation of policy measures at day  $t$ , the level of mobility affects the number of reported cases  $s$  days later (path  $\psi_{ks}$ ). Hence, each policy measure has an immediate effect on mobility, which is transferred into a delayed indirect effect on the reported number of new cases through mobility (the product of paths  $\beta_l^{(k,s)}$  and  $\psi_{ks}$ ). Each policy measures also has a direct effect on the number of reported cases via behavioral adaptions not related to mobility. This effect is also subject to a lag of  $s$  days (path  $\lambda_l^{(k,s)}$ ).

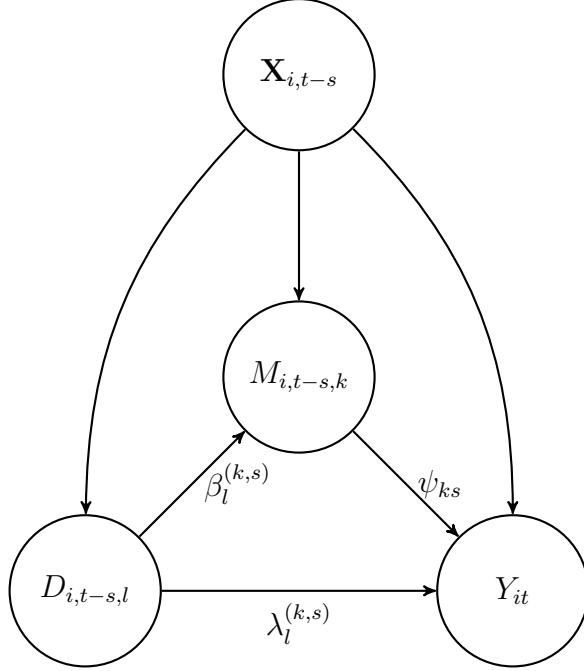


Figure 23: A directed acyclic graph of the structural equation model within a fixed point in time. The vector  $\mathbf{X}_{i,t-s}$  denotes the weekday, time, and canton effects in the models.

Note that every time-varying variable in the mediation model is lagged by  $s$  days, but that in the outcome model, only the mobility variable and the policy measures are subject to this lag. With this specification, we estimate how the instantaneous effect of the policy measures on mobility variable  $k$  in day  $t - s$  affect the number of reported new cases in day  $t$  directly and indirectly via mobility.

For estimation, we allow the canton random effects  $\boldsymbol{\theta}^{(k,M)} = (\theta_1^{(k,s,M)}, \dots, \theta_N^{(k,s,M)})$  and  $\boldsymbol{\theta}^{(k,s,Y)} = (\theta_1^{(k,s,Y)}, \dots, \theta_N^{(k,s,Y)})$  of the mediator model and outcome model, respectively, to be correlated. We thereby account for possible correlation between the baseline relative mobility and baseline relative (reported) infection risk across cantons. We achieve this by modeling the random

effects as drawn from a bivariate Gaussian distribution:

$$\begin{bmatrix} \boldsymbol{\theta}^{(k,s,M)} \\ \boldsymbol{\theta}^{(k,s,Y)} \end{bmatrix} \sim \text{MVN}(\mathbf{0}, \boldsymbol{\Omega}_{M,Y}), \quad \boldsymbol{\Omega}_{M,Y} = \begin{bmatrix} \sigma_{\boldsymbol{\theta}^{(k,s,M)}}^2 \mathbf{I} & \sigma_{\boldsymbol{\theta}^{(k,s,M)} \boldsymbol{\theta}^{(k,s,Y)}} \mathbf{I} \\ \sigma_{\boldsymbol{\theta}^{(k,s,Y)} \boldsymbol{\theta}^{(k,s,M)}} \mathbf{I} & \sigma_{\boldsymbol{\theta}^{(k,s,Y)}}^2 \mathbf{I} \end{bmatrix} = \boldsymbol{\Sigma}_{M,Y} \otimes \mathbf{I}. \quad (24)$$

Here,  $\sigma_{\boldsymbol{\theta}^{(k,s,M)}}^2$  and  $\sigma_{\boldsymbol{\theta}^{(k,s,Y)}}^2$  is the cross-canton variance of the random effect of the mediation model and outcome model  $(k, s)$ , respectively, and the off-diagonal term is the cross-canton covariance between the models' respective random effects. The  $2 \times 2$  covariance matrix  $\boldsymbol{\Sigma}_{M,Y}$  contains these variance and covariance terms. Computing the Pearson correlation coefficient

$$\rho_{\boldsymbol{\theta}^{(k,s,M)} \boldsymbol{\theta}^{(k,s,Y)}} = \frac{\sigma_{\boldsymbol{\theta}^{(k,s,M)} \boldsymbol{\theta}^{(k,s,Y)}}}{\sqrt{\sigma_{\boldsymbol{\theta}^{(k,s,M)}}^2 \sigma_{\boldsymbol{\theta}^{(k,s,Y)}}^2}} \quad (25)$$

then gives the correlation between the random effects of mediation model and outcome model  $(k, s)$ . The correlation coefficient is in turn the off-diagonal element in the  $2 \times 2$  correlation matrix  $\mathbf{R}_{M,Y}$  that corresponds to the covariance matrix  $\boldsymbol{\Sigma}_{M,Y}$ .

We estimate the structural equation model separately for mobility and the policy measures lagged by 7–13 days to see how the direct, indirect and total effects vary across the delay of the effects. To save space, however, we only estimate the models with the total trips mobility variable as a mediator.

## F.2 Identification

We now state the identification conditions and assumptions required for the mediation analysis. Imai et al.<sup>84,85</sup> propose a “sequential ignorability” assumption under which the direct and indirect effects are identified if the structural equation model is linear and contains no treatment-mediator interaction. The assumption consist of two parts. In the setting of this study, the assumptions are:

(1) each policy measure is implemented independently of mobility and the reported number of new cases, and (2) within observations with the same status on the policy measures, the number of trips on the mobility variable is independent of the potential number of reported cases. The first part of the assumption means that the control variables, the fixed effects, and the random effects in the models are sufficient to remove any confounding in the relationships between the policy measures and mobility as well as any confounding in the relationships between policy measures and the reported number of new cases. The second part of the assumption implies that, if we also condition on the policy measures, there is no confounding of the relationship between mobility and the reported number of new cases. This is a stronger assumption since it must hold for every observed combination of the policy measures in the data. Another assumption necessary for identifying indirect effects is that the mediator is measured without error. Since our data cover every trip made with a mobile device the assumption likely holds in this study.

### F.3 Results of mediation analysis

The results from the mediation analysis with total trips as a mediator are shown in Figure 24.

**Direct effects.** The ban on gatherings of more than 5 people has the strongest estimated direct effect on the reduction in the reported number of new cases. Its estimated 95 % credible intervals range between a reduction of 18.8–38.7 % (at a lag of 13 days) to a reduction of 35.9–50.5 % (at a lag of 8 days). The credible interval of the direct effect of bans on gatherings of more than 100 people includes zero for lags 7–8 days. Hence, bans on larger gatherings may have a longer delayed direct effects than bans on smaller gatherings. Border closures do not appear to have directly reduced the reported number of new cases.

**Indirect effects.** The estimated indirect effects show that mobility mediates the effects of policy measures on the reported number of new cases. The largest indirect effects are found for venue closures and bans on gatherings of more than 5 people. Both policy measures are estimated to have reduced the reported case growth with around 6–8 % at the higher order lags indirectly

via mobility. Of particular interest is the estimated indirect effect for border closures. Recall that the estimated direct effects of border closures include zero. Hence, this implies that the effect of border closures occurs exclusively through mobility. This is to be expected considering that border closures may not affect other types of behavior than mobility.

**Total effects.** Combining the direct effects and indirect effects gives the total effects. Again, bans on gatherings of more than 5 people, bans on gatherings of more than 100 people, and school closures have the largest estimated total effects, in part due to their pronounced indirect effects. For any of the days that schools were closed, the estimates imply that there would on average be 21.2 % (95 % CrI: 9.48–32.3 %) more reported cases at the 10th day ahead and 34.1 % (95 % CrI: 24.3–42.9 %) more reported cases at the 13th day ahead if schools would instead have remained open. Note that for several lags, the indirect effect of venue closures makes up more than a third of its total effect.

Overall, the mediation analysis demonstrates that the effects of social distancing policies operate – to a large degree – through mobility. Hence, telecommunication data provides valuable information for estimating effects of policy measures aimed at reducing mobility.

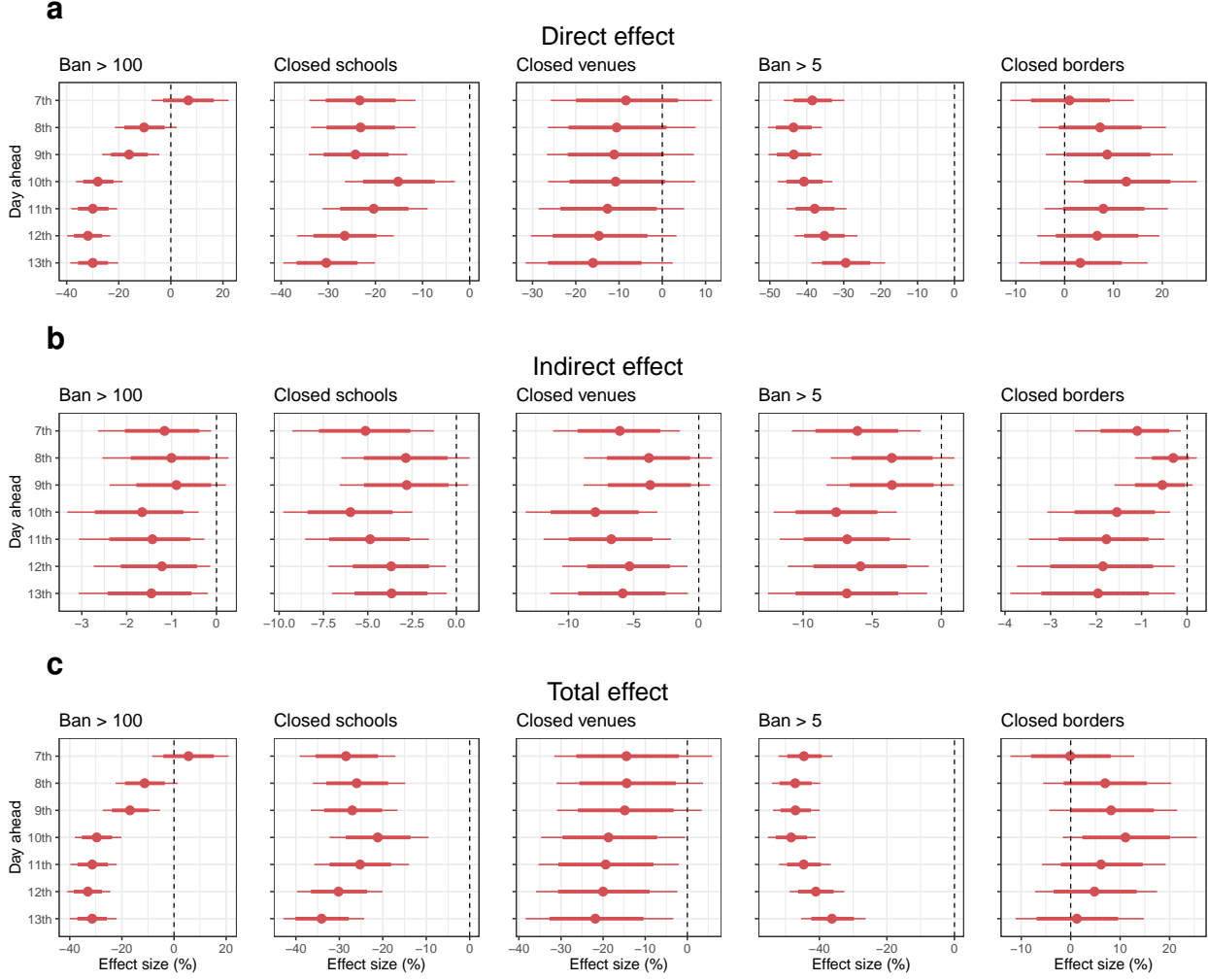


Figure 24: Mobility mediates the effect of policy measures on the reported number of new cases. Estimated **(a)** direct effect of policy measures, **(b)** indirect effect of policy measures via total trips, and **(c)** total effect of policy measures on the 7th to 13th day ahead. Posterior means are shown as dots, while 80 % and 95 % credible intervals are shown as thick and thin bars, respectively. Policy measures are arranged from top to bottom in the order in which they were implemented (cf. Supplement A).

#### F.4 Sensitivity analysis for the assumption of no unmeasured confounding

The mediation analysis rests on the sequential ignorability assumption of no unmeasured confounding in both the mediation model and the outcome model. Now, if there exists unobserved confounders that affect both the mediator and the outcome, then those variables will be part of

both models' error terms. Hence, under the assumption of no unmeasured confounding, there should be no correlation between the models' respective errors. Based on this observation, Imai et al.<sup>85</sup> propose a sensitivity analysis based on the correlation between the residuals in the two models.

To conduct the sensitivity analysis, we draw 4000 samples (e.g., as many as the length of the parameters' Markov chains, including the warm-up) from the models' predictive posterior distributions, each of the same size as the number of observations in the data. For each of the models, we subtract these values from the observed responses to get posterior samples of the model's predictive errors. We then compute the Pearson correlation coefficient between the mediation model's predictive errors and the outcome model's predictive errors for each of the 4000 posterior error samples.

Figure 25 shows kernel density estimates of the Pearson correlation coefficient distributions. The mean correlation coefficient is for each lag close to zero with the 95 % credible intervals covering zero. Hence, the sensitivity analysis suggests that there is no unmeasured confounding in the mediation analysis.

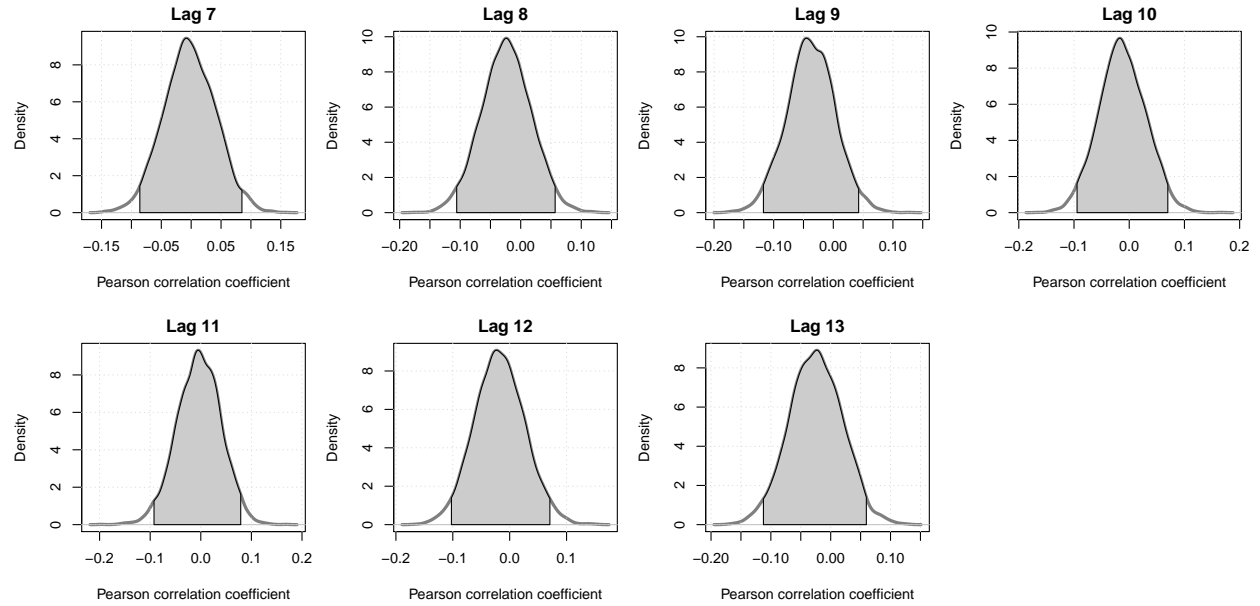


Figure 25: Kernel density estimates of the distribution of Pearson correlation coefficients between posterior samples of the mediation model's and outcome model's respective predictive errors. The shaded regions are 95 % credible intervals computed as the the area between the 2.5th and 97.5th percentile Pearson correlation coefficient.

## G Estimation details for modeling extensions and mediation analysis

Table 5 shows our choices of prior distributions for the parameters in the extended models. The new parameters are (1) the parameters for the direct effects in the mediation analysis, (2) the ICAR parameters in the spatial model, (3) the correlation coefficients for the dependence between the canton random effects in the outcome model and mediation model, and (4) the correlation coefficients for the dependence between the canton random effects in the multivariate mobility model. Below we explain the priors for the new parameters. The remaining priors are explained in Section 1.

As in the main paper, the prior on  $\beta_l$  reflects that we expect each policy measure to reduce log expected trips by on average 25 %. The prior on the direct effect parameter  $\lambda_l$  means that we expect each policy measure to reduce the log expected number of reported cases with on average 25 % conditional on mobility, with a variance such that increases in reported cases due to the policy measures are unlikely. Moreover, the prior on the mean and variance of  $\psi_{ks}$  implies that we expect mobility to predict half as large reduction in cases once we condition on the policy measures, but that negative parameter estimates are still unlikely. Note that in the spatially extended model, the canton random effects are assigned a prior of  $N(0, 1)$  due to the BYM2 reparametrization and scaling of the combined canton and spatial random effects. Moreover, the prior on the spatial random effects is technically on its conditional distribution given its neighbouring cantons spatial random effects, not its marginal distribution as it is for simplicity written in Table 5. The ICAR parameters are assigned priors according to the recommendations by Morris<sup>77</sup> and Gelman et al.<sup>86</sup>. The prior on the canton random effects correlations is, per the standard procedure in Stan, assigned on the Cholesky factor of the correlation matrix. We assign a LKJ correlation distribution with a shape parameter of 2 which makes extreme correlations less likely. All variables that are also included in the non-extended models are given the same priors as in those models, see Table 1 in

the paper. The ICAR model is estimated via the implementation available in the `brms` package. See<sup>78</sup> for details.

Parameter	Description	Prior	Model
$\beta_l$	Policy measure $l$	$N(-0.25, 0.25)$	(13), (20)
$\lambda_l$	Policy measure $l$	$N(-0.25, 0.125)$	(21)
$\psi_{ks}$	Log mobility variable $k$ with a lag of $s$	$N(0.5, 0.125)$	(21)
$\theta_i$	Canton random effect	$N(0, \sigma_\theta)$	(20), (21), (18)
$\sigma_\theta$	Standard deviation for canton random effect	Half-t(3, 0, 2.5)	(20), (21), (18)
$\theta_i$	Canton random effect in the spatial model	$N(0, 1)$	(13)
$\alpha$	Intercept	Half-t(3, 1.8, 2.5)	All
$\delta_{w(t)}$	Weekday $w$ compared to Monday	$N(0, 0.5)$	All
$\gamma$	Log no. of days since 1st reported case	$N(1, 1)$	All
$\gamma_B$	Between-canton average of log no. of days since 1st reported case	$N(0, 5)$	All
$\psi_{ks,B}$	Between-canton average of log mobility with a lag of $s$	$N(0, 5)$	(21)
$\zeta$	Overdispersion in dependent variable	Gamma(0.01, 0.01)	All
$\phi_i$	Spatial random effect	ICAR model (14)	(13)
$\varphi$	ICAR mixing parameter	Beta(0.5, 0.5)	(13)
$\tau^{-0.5}$	ICAR standard deviation	Half-t <sub>3,0,2.5</sub>	(13)
$\mathbf{R}_{M,Y}$	Cross-mediation-outcome random effect correlation matrix	LKJ(2)	(24)
$\mathbf{R}_M$	Cross-mobility variable random effect correlation matrix	LKJ(2)	(18)

*Note:* The superscripts  $(k)$  and  $(k, s)$  are omitted as the same priors are assigned to each model. The column “Description” states what effect the associated parameter represent (except for the overdispersion parameter).

Table 5: **Choice of priors for all models**